Available online at www.sciencedirect.com
ScienceDirect
Journal of Differential Equations 343 (2023) 495–529
Journal of Differential Equations
www.elsevier.com/locate/jde

Bifurcations in Holling-Tanner model with generalist predator and prey refuge ☆

Chuang Xiang [a], Jicai Huang [a,*], Hao Wang [b,*]

[a] School of Mathematics and Statistics & Hubei Key Laboratory of Mathematical Sciences, Central China Normal University, Wuhan, Hubei 430079, PR China

[b] Department of Mathematical and Statistical Sciences, University of Alberta, Edmonton, Alberta T6G 2G1, Canada

Received 20 July 2022; accepted 12 October 2022

Abstract

Refuge provides an important mechanism for preserving many ecosystems. Prey refuges directly benefit prey but also indirectly benefit predators in the long term. In this paper, we consider the complex dynamics and bifurcations in Holling-Tanner model with generalist predator and prey refuge. It is shown that the model admits a nilpotent cusp or focus of codimension 3, a nilpotent elliptic singularity of codimension at least 4, and a weak focus with order at least 3 for different parameter values. As the parameters vary, the model can undergo three types degenerate Bogdanov-Takens bifurcations of codimension 3 (cusp, focus and elliptic cases), and degenerate Hopf bifurcation of codimension 3. The system can exhibit complex dynamics, such as multiple coexistent periodic orbits and homoclinic loops. Moreover, our results indicate that the constant prey refuge prevents prey extinction and causes global coexistence. A preeminent finding is that refuge can induce a stable, large-amplitude limit cycle enclosing one or three positive steady states. Numerical simulations are provided to illustrate and complement our theoretical results.

MSC: primary :34C23, 34C25; secondary 34C37, 92D25S

Keywords: Holling-Tanner model; Generalist predator; Constant prey refuge; Bogdanov-Takens bifurcation; Hopf bifurcation; Coexistence

☆ Research was partially supported by NSFC (No. 11871235, 12231008) and NSERC (RGPIN-2020-03911 and RGPAS-2020-00090).

* Corresponding authors.
E-mail addresses: hjc@mail.ccnu.edu.cn (J. Huang), hao8@ualberta.ca (H. Wang).

https://doi.org/10.1016/j.jde.2022.10.018
0022-0396/

1. Introduction

Refuges, for instance coral reefs, are critical in the preservation and persistence of an ecosystem. Prey can stay in a refuge to escape from predation, while predators can also benefit from the prey refuge effect in the long term. Clearly prey refuges facilitate the coexistence of prey and predators in a habitat [4,25]. Motivated by three typical ecosystems, Wang et al. [36] quantitatively formulated and explored three mechanisms of refuge-mediated prey-predator interactions that lead to paradoxical inverted biomass pyramids. Gause et al. [13] constructed a Filippov predator-prey model to describe the effect of the prey refuge. Prey refuges were widely believed to have two most significant roles: preventing prey extinction and damping predator-prey oscillations [27]. The former one was confirmed by some empirical evidences, but the latter was still in doubt [27,28]. Moreover, McNair [27] found that several kinds of refuges can exert a locally destabilizing effect and create stable, large-amplitude oscillations which would damp out if no refuge was present. McNair [28] found that a prey refuge with legitimate entry-exit dynamics is quite capable of amplifying rather than damping predator-prey oscillations. The methodology of incorporating prey refuges into predator-prey models were various [27,28,31,34,35]. As a basic topic in ecology, researchers have extensively investigated the effects of prey refuge on the predator-prey dynamics [5,18,20,26,29].

To introduce our model, we start from the general Leslie type predator-prey system as follows (Freedman and Mathsen [11]):

$$\begin{aligned}\dot{x} &= (\rho_1 - b_1 x)x - p(x)y,\\ \dot{y} &= (\rho_2 - \frac{a_2 y}{x})y,\end{aligned} \tag{1.1}$$

where $x(t)$ and $y(t)$ denote densities of prey and predators at time t, respectively; and $p(x)$ is the so-called functional response describing the per capita consumption rates of predators depending on prey density. System (1.1) with different functional responses $p(x)$ has been thoroughly studied in the literature (see [12,16,17,30,38] and references therein).

Aziz-Alaoui and Okiye [3] considered generalist predator and Holling II functional response in system (1.1) as follows

$$\begin{aligned}\dot{x} &= x(\rho_1 - b_1 x) - \frac{a_1 x}{n+x}y,\\ \dot{y} &= (\rho_2 - \frac{a_2 y}{q+x})y,\end{aligned} \tag{1.2}$$

where a_1 is the maximum rate of predation, and n is the half-saturation constant. Here $x+q$ is the new carrying capacity for predators, and $q>0$ can be seen as an extra constant carrying capacity coming from all the other food sources for predators. Note that when $x=0$, the second equation in system (1.2) becomes $\dot{y} = (\rho_2 - \frac{a_2 y}{q})y$, that is the predator can survive by switching to other food source even its favorite prey disappears. Thus, the predators in system (1.2) can be regarded as a generalist predator. System (1.2) and its variations have been studied extensively, see for example, Aziz-Alaoui and Okiye considered the boundedness of solutions, the existence of an attracting set, and global stability of the coexisting interior equilibrium of system (1.2) [3]. Later Li and Song [23] made a detailed study about the global stability of the unique positive equilibrium of system (1.2). Recently, Xiang, Huang and Wang [38] showed the existence of degenerate Bogdanov-Takens bifurcation of codimension 3 (cusp case) and Hopf bifurcation with codimension at most 2. Moreover, they showed that the prey population can go extinct for some positive initial densities.

The simplest yet important refuge is the constant prey refuge, which is assumed to be a constant (say μ). When the prey population is below the quantity μ, the predators cannot capture prey, whereas when the prey population is above this quantity, predation takes place. Recently, Slimani *et al.* [32] considered a constant prey refuge in model (1.2) as follows:

$$\begin{aligned}\dot{x} &= x(\rho_1 - b_1 x) - \frac{a_1 (x-\mu)_+}{n + (x-\mu)_+} y,\\ \dot{y} &= y(\rho_2 - \frac{a_2 y}{q + (x-\mu)_+}),\end{aligned} \tag{1.3}$$

where $(x-\mu)_+ = \max\{0, x-\mu\}$, and $\mu \geq 0$ represents the constant refuge of prey and leaves $(x-\mu)_+$ of the prey available to the predator. When the predator is absent, the density of prey x satisfies a logistic equation and converges to $\frac{\rho_1}{b_1}$. For system (1.3), there exists a certain threshold values μ such that, if $x > \mu$, i.e., the density of prey is relatively high, then the prey could go out of the refuge to seek food since most food sources for prey to survive are outside the refuge, hence $(x-\mu)_+ = x - \mu$; if $x < \mu$, i.e., the density of pres is relatively low and the prey will stay in the refuge, then $(x-\mu)_+ = 0$. The attracting set, the existence and rough types of positive equilibria, globally asymptotical stability of a unique positive equilibrium, the existence of limit cycles were studied in [32]. However, the biological effect of constant prey refuge, the complex dynamical behaviors and bifurcation phenomena still remain unknown, especially for the high codimension bifurcations in system (1.3).

In this paper, we revisit system (1.3) for the case $\mu > 0$. We perform the classification of positive equilibria of system (1.3). By the normal form theory, we will show that system (1.3) has three types nilpotent positive equilibria: cusp and focus with codimension at most 3, elliptic with codimension at least 4, and system (1.3) can undergo three different types degenerate Bogdanov-Takens bifurcations of codimension 3 (cusp, focus and elliptic cases). For the Hopf bifurcation problem, using the resultant elimination and pseudo-division to solve the semi-algebraic varieties of focal values, we will prove that the order of a weak focus of system (1.3) is at least 3, and system (1.3) can undergo degenerate Hopf bifurcation of codimension 3. Moreover, we will further prove that all the boundary equilibria of system (1.3) are unstable, which implies as t tends to $+\infty$, prey and predators with positive initial population densities will eventually coexist in the form of periodic oscillations or positive steady states.

For simplicity, we first nondimensionalize system (1.3) with the following scaling:

$$x = \frac{\rho_1}{b_1}\overline{x}, \quad y = \frac{\rho_1 \rho_2}{b_1 a_2}\overline{y}, \quad t = \frac{\tau}{\rho_1},$$

dropping the bar and still denoting τ by t for convenience leads to

$$\begin{aligned}\dot{x} &= x(1-x) - \frac{ay(x-b)_+}{k_1 + (x-b)_+},\\ \dot{y} &= cy(1 - \frac{y}{k_2 + (x-b)_+}),\end{aligned} \tag{1.4}$$

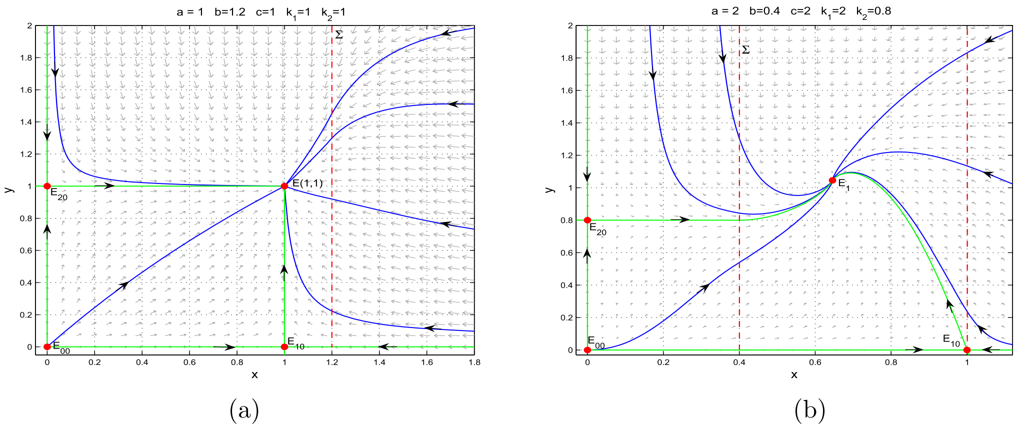

Fig. 2.1. Phase portraits of system (1.4). (a) $b = 1.2 > 1$. (b) $0 < b = 0.4 < 1$.

where all parameters are positive, and $a = \frac{a_1\rho_2}{a_2\rho_1}$, $b = \frac{b_1\mu}{\rho_1}$, $c = \frac{\rho_1}{\rho_2}$, $k_1 = \frac{b_1 n}{\rho_1}$, $k_2 = \frac{b_1 q}{\rho_1}$,

$$(x-b)_+ = \max\{0, x-b\}.$$

The remaining paper is organized as follows. In section 2, we study the existence of nonnegative equilibria and their types. In section 3, we analyze three different types of Bogdanov-Takens bifurcations of codimension 3 and provide some numerical simulations. The Hopf bifurcation of the center-type equilibrium corresponding to system (1.4) is studied in section 4. Finally, in section 5 we explain some important theoretical results and conclude the paper.

2. Equilibria and their types

In this section, we analyze the number and types of nonnegative equilibria of system (1.4) in $\mathbb{R}^2_+ = \{(x, y)|x \geqslant 0, y \geqslant 0\}$. Obviously, system (1.4) is locally Lipschitz and piecewise-smooth, and the positive invariant and bounded region of system (1.4) is (see Fig. 2.1)

$$\Omega = \{(x, y)|0 \le x \le 1,\ \ 0 \le y \le k_2 + \max\{0, 1-b\}\}.$$

System (1.4) is equivalent to the following two systems:

$$\begin{aligned} \dot{x} &= x(1-x), \\ \dot{y} &= cy\left(1 - \frac{y}{k_2}\right), \qquad 0 < x < b, \end{aligned} \tag{2.1}$$

and

$$\begin{aligned} \dot{x} &= x(1-x) - \frac{ay(x-b)}{k_1 + (x-b)}, \\ \dot{y} &= cy\left(1 - \frac{y}{k_2 + (x-b)}\right), \qquad x \ge b. \end{aligned} \tag{2.2}$$

Note that system (1.4) has a switching line Σ, where

$$\Sigma = \{(x, y) \in \mathbb{R}^+ \times \mathbb{R}^+ : x = b\},$$

which separates the interior of the first quadrant into two subregions

$$S_1 = \{(x, y) \in \mathbb{R}^+ \times \mathbb{R}^+ : x < b\},$$
$$S_2 = \{(x, y) \in \mathbb{R}^+ \times \mathbb{R}^+ : x > b\}.$$

System (1.4) always has three boundary equilibria $E_{00}(0, 0)$, $E_{10}(1, 0)$ and $E_{20}(0, k_2)$. Considering the corresponding Jacobian matrix of system (1.4) at these boundary equilibria, we can obtain the following results.

Lemma 2.1. *System (1.4) always has three boundary equilibria: $E_{00}(0, 0)$ is always an unstable node, $E_{10}(1, 0)$ and $E_{20}(0, k_2)$ are always hyperbolic saddles.*

2.1. Case I: $b \geq 1$ (i.e., $\mu \geq \frac{\rho_1}{b_1}$)

In this case, system (1.4) has a unique positive equilibrium $(1, k_2)$, which is always a stable hyperbolic node. Moreover, we have the following result.

Theorem 2.2. *If $b \geq 1$, then the unique positive equilibrium $(1, k_2)$ is a global attractor for system (1.4) in the interior of the first quadrant.*

Proof. When $b \geq 1$, all of the trajectories of system (1.4), starting in S_2, will cross the line $x = b$ from right to left. In the region S_1, system (1.4) becomes as system (2.1). The unique positive equilibrium $(1, k_2)$ is located on the invariant line $x = 1$ of system (2.1). Moreover, the three boundary equilibria are all unstable, and the positive invariant and bounded region of system (2.1) is $\Omega = \{(x, y)|0 \leq x \leq 1, 0 \leq y \leq k_2\}$ (see Fig. 2.1(a)). Thus the unique positive equilibrium $(1, k_2)$ is a global attractor for system (1.4) in the interior of the first quadrant. □

2.2. Case II: $0 < b < 1$ (i.e., $0 < \mu < \frac{\rho_1}{b_1}$)

In this case, all of the trajectories of system (1.4), starting in the region S_1, will cross the line $x = b$ from left to right; all of the trajectories of system (1.4), starting in the region S_2, will cross the line $x = 1$ from right to left (see Fig. 2.1(b)).

Next, we study the positive equilibria of system (1.4). In fact, we only need to focus on system (2.2). The positive equilibria satisfy the following equations:

$$\begin{cases} x(1-x) - \frac{ay(x-b)}{k_1+x-b} = 0, \\ 1 - \frac{y}{k_2+x-b} = 0, \end{cases} \tag{2.3}$$

and $x \in (b, 1)$. From (2.3), we have

$$x^3 - (1 + b - a - k_1)x^2 + ((1 - 2a)b + ak_2 - k_1)x + ab(b - k_2) = 0, \tag{2.4}$$

which have at most three positive roots, denoted as x_i $(i = 1, 2, 3)$, in the interval $(b, 1)$, correspondingly, system (2.2) can have at most three positive equilibria: $E_i(x_i, y_i)$ $(i = 1, 2, 3)$. Define

$$F(x) = x^3 - (1 + b - a - k_1)x^2 + (b(1 - 2a) + ak_2 - k_1)x + ab(b - k_2),$$
$$f(x) = \frac{dF}{dx} = 3x^2 - 2(1 + b - a - k_1)x + (b(1 - 2a) + ak_2 - k_1). \tag{2.5}$$

Through a direct calculation, we have

$$F(b) = (b - 1)bk_1 < 0, \quad F(1) = a(1 - b)(1 + k_2 - b) > 0. \tag{2.6}$$

The Jacobian matrix of system (1.4) at any positive equilibrium $E(x, y)$ takes the form:

$$J(E) = \begin{pmatrix} 1 - 2x - \frac{k_1 x(1-x)}{(x-b)(k_1+x-b)} & -\frac{x(1-x)}{k_2+x-b} \\ c & -c \end{pmatrix},$$

from which we have

$$\text{Det}(J(E)) = c\left(\frac{x(1 - x)}{k_2 + x - b} - 1 + 2x + \frac{k_1 x(1 - x)}{(x - b)(k_1 + x - b)}\right),$$
$$\text{Tr}(J(E)) = 1 - 2x - \frac{k_1 x(1 - x)}{(x - b)(k_1 + x - b)} - c.$$

Let $F(x) = 0$, then a can be solved as

$$a = \frac{x(1 - x)(k_1 + x - b)}{(x - b)(k_2 + x - b)}. \tag{2.7}$$

Substituting (2.7) into $\text{Det}(J(E))$ and $f(x)$ leads to

$$\text{Det}(J(E)) = \frac{c}{(x - b)(k_1 + x - b)} f(x). \tag{2.8}$$

According to the root formula of the third-order algebraic equation, we define

$$A = (1 + b - a - k_1)^2 - 3(b(1 - 2a) + ak_2 - k_1),$$
$$\Delta = -4A^3 + (-3(1 + b - a - k_1)A + (1 + b - a - k_1)^3 + 27ab(b - k_2))^2. \tag{2.9}$$

Since the maximum number of positive roots of (2.4) is determined by the constant term of equation (2.4), next we classify the number and type of positive equilibria of system (1.4) into the following two cases: (1) $b < k_2$ (i.e., $\mu < q$); (2) $b \geq k_2$ (i.e., $\mu \geq q$).

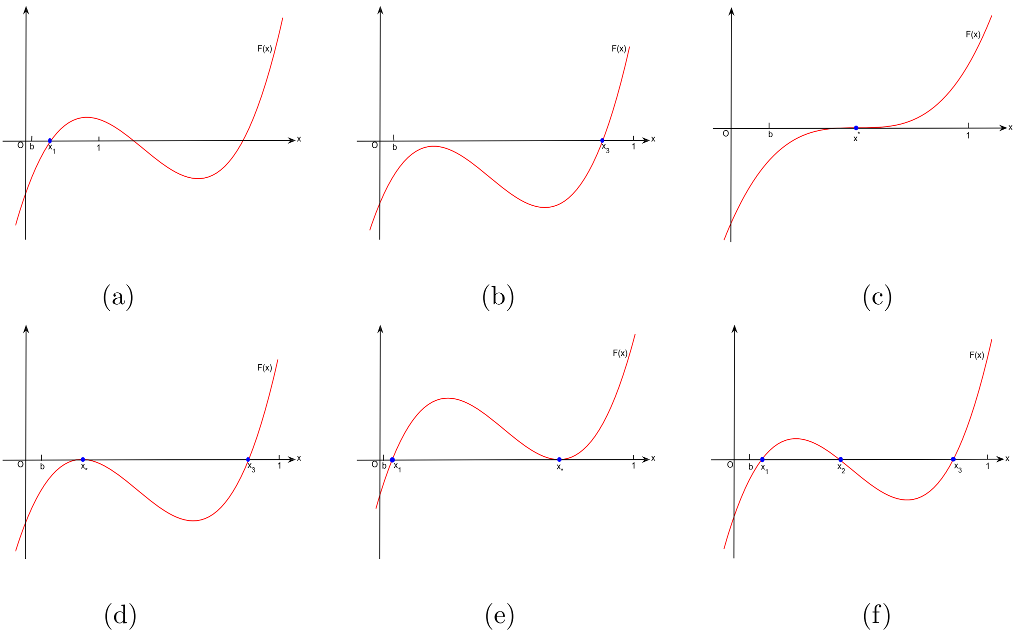

Fig. 2.2. The positive roots of $F(x) = 0$ in $(b, 1)$ when $b < \min\{1, k_2\}$. (a)(b) $F(x)$ has a single root; (c) $F(x)$ has a triple root; (d)(e) $F(x)$ has a single root and double root; (f) $F(x)$ has three distinct single roots.

2.2.1. The case of $b < k_2$ (i.e., $\mu < q$)

In this case, system (1.4) has three boundary equilibria: a hyperbolic unstable node E_{00}, two hyperbolic saddles E_{10} and E_{20}, and at most three different positive equilibria, which correspond to at most three positive roots in $(b, 1)$ (see Fig. 2.2). Thus, we have the following results.

Lemma 2.3. *When $b < \min\{1, k_2\}$, system (2.2) (or system (1.4)) has at least one positive equilibrium and at most three different positive equilibria. Moreover,*

- (I) *system (2.2) has a unique positive equilibrium if one of the following conditions is satisfied:*
  - (i) *$\Delta < 0$, and $1 < x_2 < x_3$ or $x_1 < x_2 < b$. The unique positive equilibrium $E_1(x_1, y_1)$ (or $E_3(x_3, y_3)$) is an elementary anti-saddle;*
  - (ii) *$\Delta = 0$, $A > 0$, and $x_* > 1$ or $x_* < b$. The unique positive equilibrium is E_1 or E_3;*
  - (iii) *$\Delta = A = 0$. The unique positive equilibrium $E^*(x^*, y^*)$ is degenerate;*
  - (iv) *$\Delta > 0$. The unique positive equilibrium is E_3;*
- (II) *if $\Delta = 0$, $A > 0$ and $b < x_1 < x_* < 1$ or $b < x_* < x_3 < 1$, then system (2.2) has two positive equilibria: an elementary anti-saddle E_1 (or E_3), and a degenerate equilibrium $E_*(x_*, y_*)$;*
- (III) *if $\Delta < 0$ and $b < x_1 < x_2 < x_3 < 1$, then system (2.2) has three positive equilibria: a hyperbolic saddle $E_2(x_2, y_2)$, two elementary anti-saddles E_1 and E_3.*

Proof. According to equation (2.8) and the property of $f(x)$, we have $\text{Det}(J(E_i)) > 0$ $(i = 1, 3)$, $\text{Det}(J(E_2)) < 0$, $\text{Det}(J(E_*)) = 0$ and $\text{Det}(J(E^*)) = 0$, hence E_1, E_2 and E_3 are all elementary equilibria and only E_2 is a hyperbolic saddle, E_* and E^* are both degenerate equilibria. □

We next explore the detailed types of degenerate equilibria E_* and E^* in Lemma 2.3.

Case (II) of Lemma 2.3: E_3 and E_*. we first look for some parameter values such that $E_3(x_3, y_3)$ is a nonhyperbolic equilibrium satisfying $\mathrm{Det}(J(E_3)) > 0$ and $\mathrm{Tr}(J(E_3)) = 0$, and the degenerate equilibrium $E_*(x_*, y_*)$ satisfying $\mathrm{Tr}(J(E_*)) = 0$. From $F(x_*) = f(x_*) = 0$, and $\mathrm{Det}(J(E_*)) = \mathrm{Tr}(J(E_*)) = \mathrm{Tr}(J(E_3)) = 0$, we can express a, b, k_1, k_2, y_*, x_3 and y_3 by x_* and c as follows:

$$\begin{aligned}
a &= \frac{(3x_*(x_*-1)+1-c^2)c}{2c(1-c)+(1-4c)x_*-x_*^2}, \quad b = \frac{x_*(c(1-c-x_*)+x_*^2)}{3x_*(x_*-1)+1-c^2},\\
k_1 &= \frac{x_*(1-x_*)(1-c-2x_*)^3}{(3x_*(x_*-1)+1-c^2)(2c(1-c)+(1-4c)x_*-x_*^2)},\\
k_2 &= \frac{x_*(1-x_*)(3x_*^2+(2c-3)x_*+1-c)}{c(1-c^2+3x_*(x_*-1))}, \quad y_* = \frac{x_*(1-x_*)}{c},\\
x_3 &= \frac{(1-c-x_*)(c(1-c-x_*)+x_*^2)}{2c(1-c)+x_*(1-4c)-x_*^2}, \quad y_3 = \frac{(c+x_*)^2(1-c-x_*)^2}{c(2c(1-c)+(1-4c)x_*-x_*^2)},
\end{aligned} \tag{2.10}$$

where $0 < x_* < \frac{1-c}{2}$ and $0 < c < 1$. Then we have the following results.

Theorem 2.4. *If the conditions in (2.10), $0 < x_* < \frac{1-c}{2}$ and $0 < c < 1$ hold, then system (2.2) has two positive equilibria: a cusp $E_*(x_*, y_*)$ of codimension 2, and an unstable weak focus $E_3(x_3, y_3)$ of order 1.*

Proof. First we prove E_3 is a weak focus. Make the following linear transformations successively:

$$\begin{aligned}
&x = u + x_3, \quad y = v + y_3;\\
&u = -\frac{\breve{a}_{01}\sqrt{d}}{\breve{a}_{10}^2+d}X - \frac{\breve{a}_{10}\breve{a}_{01}}{\breve{a}_{10}^2+d}Y, \quad v = Y,
\end{aligned}$$

where $d = \mathrm{Det}(J(E_3))$ and

$$\breve{a}_{10} = c, \quad \breve{a}_{01} = -\frac{c(c^2+cx_*-(x_*-1)^2)(c^2+c(x_*-1)-x_*^2)}{(c^2+c(2x_*-1)+(x_*-1)x_*)(2c^2+c(4x_*-2)+(x_*-1)x_*)}.$$

Then system (2.2) becomes (denote X and Y by x and y, respectively)

$$\dot{x} = -\sqrt{d}y + \breve{f}(x, y), \dot{y} = \sqrt{d}x + \breve{g}(x, y), \tag{2.11}$$

where

$$\begin{aligned}
\breve{f}(x, y) &= \breve{a}_{20}x^2 + \breve{a}_{11}xy + \breve{a}_{02}y^2 + \breve{a}_{30}x^3 + \breve{a}_{21}x^2y + \breve{a}_{12}xy^2 + \breve{a}_{03}y^3 + o(|x, y|^3),\\
\breve{g}(x, y) &= \breve{b}_{20}x^2 + \breve{b}_{30}x^3 + \breve{b}_{21}x^2x + o(|x, y|^3),
\end{aligned}$$

$\breve{a}_{ij}$ and $\breve{b}_{ij}$ can be expressed by c and x_*, to save space, here we omit them. According to the formula of First Lyapunov number [6]

$$\begin{aligned}\sigma_1 &= \frac{1}{16}(\check{f}_{xxx}+\check{f}_{xyy}+\check{g}_{xxy}+\check{g}_{yyy}\\ &\quad+\frac{\check{f}_{xy}(\check{f}_{xx}+\check{f}_{yy})-\check{g}_{xy}(\check{g}_{xx}+\check{g}_{yy})-\check{f}_{xx}\check{g}_{xx}+\check{f}_{yy}\check{g}_{yy}}{\sqrt{d}})|_{x=y=0}\\ &=\frac{1}{16}(6\check{a}_{30}+2\check{a}_{12}+2\check{b}_{21}+\frac{2\check{a}_{11}(\check{a}_{20}+\check{a}_{02})-4\check{a}_{20}\check{b}_{20}}{\sqrt{d}})\\ &=-\frac{x_*(1-x_*)R_{01}(x_*)}{8(1-c-2x_*)(c+x_*)^4(1-c-x_*)^4},\end{aligned}$$

where

$$\begin{aligned}R_{01}(x_*) &= 3x_*^6+(30c-9)x_*^5+(75c^2-75c+9)x_*^4+3(36c^3-50c^2+20c-1)x_*^3\\ &\quad+c(95c^3-162c^2+82c-15)x_*^2+c^2(c-1)^2(44c-7)x_*+2c^2(c-1)^3(4c+1).\end{aligned}$$

Since $0<x_*<\frac{1-c}{2}$ and $0<c<1$, then all the factors except $R_{01}(x_*)$ of σ_1 are greater than zero. Note that $R_{01}(0)=-2c^2(1+4c)(1-c)^3<0$ and $R_{01}(\frac{1-c}{2})=-\frac{3(1-c^2)^3}{64}<0$. Hence, for any $c\in(0,1)$, Lemma 3.1 in Yang [39] indicates that the number of roots for $R_{01}(x_*)$ in interval $(0,\frac{1-c}{2})$ is equal to that of positive roots for

$$\Phi_1(x_*)=(1+x_*)^6R_{01}(\frac{1-c}{2(1+x_*)})=-\frac{(1-c)^3}{64}\phi(x_*),$$

where

$$\begin{aligned}\phi(x_*) &= 128(1+4c)c^2x_*^6+32(31+52c)x_*^5+48(5+41c+45c^2)cx_*^4+8(3+60c+214c^2\\ &\quad+172c^3)x_*^3+4(9+84c+182c^2+107c^3)x_*^2+6(3+10c)(1+c)^2x_*+3(1+c)^3.\end{aligned}$$

Obviously $\phi(x_*)>0$ for any $x_*>0$, which means $\Phi_1(x_*)<0$ for $x_*>0$, i.e., $\Phi_1(x_*)$ has no positive root. Hence, $R_{01}(x_*)<0$ hold for $0<x_*<\frac{1-c}{2}$ and $0<c<1$, then $\sigma_1>0$, which implies E_3 is an unstable weak focus of order one.

Next we prove that if the conditions in (2.10) hold, then E_* is a cusp of codimension 2. We first make the following linear transformations successively:

$$x=u+x_*,\quad y=v+y_*;\quad u=X+\frac{Y}{c},\quad v=X,$$

then system (2.2) becomes

$$\begin{aligned}\dot{X} &= Y-\frac{1}{x_*(1-x_*)}Y^2+o(|X,Y|^2),\\ \dot{Y} &= \frac{c^2(1-c-2x_*)}{x_*(1-x_*)}X^2+\frac{3c(1-c-2x_*)}{x_*(1-x_*)}XY+\frac{2-c-4x_*}{x_*(1-x_*)}Y^2+o(|X,Y|^2),\end{aligned}\tag{2.12}$$

and according to Lemma 3.1 in Huang et al. [15], we know that system (2.12) is equivalent to

$$\begin{aligned}\dot{x} &= y + o(|x, y|^2),\\ \dot{y} &= \frac{c^2(1-c-2x_*)}{x_*(1-x_*)}x^2 + \frac{3c(1-c-2x_*)}{x_*(1-x_*)}xy + o(|x, y|^2).\end{aligned} \tag{2.13}$$

$\frac{c^2(1-c-2x_*)}{x_*(1-x_*)} \neq 0$ and $\frac{3c(1-c-2x_*)}{x_*(1-x_*)} \neq 0$ since $0 < x_* < \frac{1-c}{2}$. Hence, E_* is cusp of codimension 2. □

Case (II) of Lemma 2.3: E_1 and E_*. Define

$$\begin{aligned}C_r(x_*, c) :=\ &(c-2)(c-1)^4c^3 + 4(3c^2-4c-4)(c-1)^3c^2x_*\\ &+ 4(c-1)^2(13c^3-c^2-38c+6)cx_*^2\\ &+ 8(9c^4+26c^3-117c^2+112c-30)cx_*^3 - 8(13c^4-135c^3+221c^2-105c+6)x_*^4\\ &- 48(9c^3-33c^2+28c-4)x_*^5 - 48(11c^2-21c+6)x_*^6 + 96(2-3c)x_*^7 - 48x_*^8,\end{aligned} \tag{2.14}$$

and

$$\begin{aligned}h(c) &:= \sqrt{2c(1+c)}, \quad a_2 := -\frac{c(c^2+c(6x_*-3)+6x_*^2-6x_*+2)}{c^2+c(2x_*-1)+2(x_*-1)x_*},\\ b_2 &:= \frac{x_*(c^2+c(4x_*-1)+2x_*^2)}{c^2+c(6x_*-3)+6x_*^2-6x_*+2},\\ k_{22} &:= \frac{(1-x_*)x_*(3c^2+5c(2x_*-1)+6x_*^2-6x_*+2)}{c(c^2+c(6x_*-3)+6x_*^2-6x_*+2)},\\ k_{12} &:= -\frac{4(x_*-1)x_*(c+2x_*-1)^3}{(c^2+c(2x_*-1)+2(x_*-1)x_*)(c^2+c(6x_*-3)+6x_*^2-6x_*+2)}.\end{aligned} \tag{2.15}$$

Lemma 2.5. *Assume $\frac{h(c)-2c}{2} < x_* < \frac{1-c}{2}$ and $0 < c < 1$, then $C_r(x_*, c) < 0$.*

Proof. If we take c as a parameter, then $C_r(x_*, c)$ can be regarded as a function of degree 8 with respect to x_*. By straightforward calculation, we can get $C_r(\frac{h(c)-2c}{2}, c) < 0$ and $C_r(\frac{1-c}{2}, c) < 0$ for any $c \in (0, 1)$. Lemma 3.1 in Yang [39] indicates that the number of roots for $C_r(x_*, c)$ in the interval $(\frac{h(c)-2c}{2}, \frac{1-c}{2})$ is equal to that of positive roots for

$$\begin{aligned}\Phi_2(x_*) &= (1+x_*)^8 C_r\left(\frac{1-c+(h(c)-2c)x_*}{2(1+x_*)}, c\right)\\ &= \phi_0 + \phi_1x_* + \phi_2x_*^2 + \phi_3x_*^3 + \phi_4x_*^4 + \phi_5x_*^5 + \phi_6x_*^6 + \phi_7x_*^7 + \phi_8x_*^8,\end{aligned}$$

where ϕ_i are given in Appendix A.

By Sturm's Theorem we can prove that $\phi_i < 0$ $(i = 0, 1, 2, 3, 4, 5, 6, 7, 8)$ for $c \in (0, 1)$. Hence, $\Phi_2(x_*) < 0$, which implies $\Phi_2(x_*)$ has no positive root. Thus $C_r(x_*, c) < 0$ for $\frac{h(c)-2c}{2} < x_* < \frac{1-c}{2}$ and $0 < c < 1$. □

Theorem 2.6. *If* $(a, b, k_1, k_2) = (a_2, b_2, k_{12}, k_{22})$, $\frac{h(c)-2c}{2} < x_* < \frac{1-c}{2}$ *and* $0 < c < 1$, *then system* (2.2) *has two positive equilibria: a stable hyperbolic focus (or node)* $E_1(x_1, k_{22} + x_1 - b_2)$, *and a cusp* $E_*(x_*, \frac{x_*(1-x_*)}{c})$ *of codimension* 3.

Proof. When $(a, b, k_1, k_2) = (a_2, b_2, k_{12}, k_{22})$, $\frac{h(c)-2c}{2} < x_* < \frac{1-c}{2}$ and $0 < c < 1$, we have

$$\begin{aligned}
\mathrm{Det}(J(E_1)) &= \frac{c^3(c+2x_*-1)^3}{(c^2+2cx_*-c-2x_*^2+2x_*)(c^2+2cx_*-c+2x_*^2-2x_*)} > 0,\\
\mathrm{Tr}(J(E_1)) &= -\frac{3c^2(c+2x_*-1)^3}{(c^2+2cx_*-c-2x_*^2+2x_*)(c^2+2cx_*-c+2x_*^2-2x_*)} < 0. \quad (2.16)
\end{aligned}$$

Hence, E_1 is a stable focus (or node).

Moreover, the Jacobian matrix of system (2.2) at E_* has two zero eigenvalues, and system (2.2) can be rewritten as

$$\begin{aligned}
\dot{u} &= \breve{a}_{10}u + \breve{a}_{01}v + \breve{a}_{20}u^2 + \breve{a}_{11}uv + \breve{a}_{30}u^3 + \breve{a}_{21}u^2v + \breve{a}_{40}u^4 + \breve{a}_{31}u^3v + o(|u, v|^4),\\
\dot{v} &= \breve{b}_{10}u + \breve{b}_{01}v + \breve{b}_{20}u^2 + \breve{b}_{11}uv + \breve{b}_{02}v^2 + \breve{b}_{30}u^3 + \breve{b}_{21}u^2v + \breve{b}_{12}uv^2 + \breve{b}_{40}u^4 + \breve{b}_{31}u^3v\\
&\quad + \breve{b}_{22}u^2v^2 + o(|u, v|^4),
\end{aligned} \quad (2.17)$$

where $\breve{a}_{ij}$ and $\breve{b}_{ij}$ can be expressed by c and x_*, here we omit them to save space.

Next following the steps in Huang et al. [15] (see also [1,2,24]), we can rewrite system (2.17) as

$$\begin{aligned}
\dot{x} &= y,\\
\dot{y} &= x^2 + \bar{M}x^3y + o(|x, y|^4),
\end{aligned} \quad (2.18)$$

where

$$\bar{M} = \frac{C_r(x_*, c)}{4c^2\sqrt{x_*^5(1-x_*)^5(1-c-2x_*)^3}},$$

from Lemma 2.5 we can know that $C_r(x_*, c) < 0$ when $\frac{h(c)-2c}{2} < x_* < \frac{1-c}{2}$ and $0 < c < 1$, which implies $\bar{M} < 0$. Hence, E_* is a cusp of codimension 3. □

Case $(I)(iii)$ **of Lemma 2.3**: system (2.2) has a unique positive equilibrium $E^*(x^*, y^*)$. From $F(x^*) = f(x^*) = 0$ and the relationship between root and coefficient, we can express a, k_1 and k_2 by x^* and b as follows

$$\begin{aligned}
a &= \frac{(3x^{*2} - 3x^* + 1)b - x^{*3}}{b(1-b)}, \quad k_1 = \frac{(x^* - b)^3}{b(1-b)},\\
k_2 &= \frac{(1-2b)x^{*3} + 3bx^{*2} - 3b^2x^* + b^2}{3bx^*(x-1) + b - x^{*3}}.
\end{aligned} \quad (2.19)$$

Moreover, from $\mathrm{Tr}(J(E^*) = 0$ and (2.19) we can obtain

$$b_0 = \frac{x^{*2}(x^* + c)}{3x^{*2} - (3 - 2c)x^* + 1 - c}, \tag{2.20}$$

then (2.19) can be simplified as follows

$$a = \frac{c(3x^{*2} + (2c - 3)x^* + 1 - c)}{(c + x^*)(1 - c - x^*)}, \quad k_1 = \frac{x^*(1 - x^*)(1 - c - 2x^*)^3}{(c + x^*)(1 - c - x^*)(3x^{*2} + (2c - 3)x^* + 1 - c)},$$

$$k_2 = \frac{x^*(1 - x^*)(3x^{*2} + (4c - 3)x^* + (1 - c)^2)}{c(3x^{*2} + (2c - 3)x^* + 1 - c)}, \tag{2.21}$$

where $0 < x^* < \frac{1-c}{2}$ and $0 < c < 1$.

Define

$$\begin{aligned}
&\mathcal{C}(x^*, c) := c(1 - c - 2x^*)^3 - 8x^*(c + x^*)(1 - x^*)(1 - c - x^*),\\
&\mathcal{P}_+ := \left\{(x^*, c)|\mathcal{C}(x^*, c) > 0,\ 0 < x^* < \frac{1 - c}{2},\ 0 < c < 1\right\},\\
&\mathcal{P}_- := \left\{(x^*, c)|\mathcal{C}(x^*, c) < 0,\ 0 < x^* < \frac{1 - c}{2},\ 0 < c < 1\right\},\\
&\mathcal{P}_0 := \left\{(x^*, c)|\mathcal{C}(x^*, c) = 0,\ 0 < x^* < \frac{1 - c}{2},\ 0 < c < 1\right\},
\end{aligned} \tag{2.22}$$

then we have the following results.

Theorem 2.7. *If $\Delta = A = 0$ and the conditions in (2.19) hold, then system (2.2) has a unique positive equilibrium E^*. Moreover,*

- (I) *E^* is a stable (or unstable) degenerate node of codimension 2 if $0 < b < b_0$ (or $b_0 < b < k_2$);*
- (II) *if $b = b_0$ and $(x^*, c) \in \mathcal{P}_-$ (or $(x^*, c) \in \mathcal{P}_+$), then E^* is a nilpotent focus (or elliptic singularity) of codimension 3;*
- (III) *if $b = b_0$ and $(x^*, c) \in \mathcal{P}_0$, then E^* is a nilpotent elliptic singularity of codimension at least 4.*

Proof. (I) When $b \neq b_0$, the Jacobian matrix of system (2.2) at E^* has a zero eigenvalue. First, we make the following linear transformations successively

$$x = X + x^*, \quad y = Y + y^*; \quad X = x + \frac{b(3x^{*2} - 3x^* + 1) - x^{*3}}{c(x^{*2} - 2bx^* + b)}y, \quad Y = x + y,$$

$$t = \frac{b(3x^{*2} + (2c - 3)x^* + 1 - c) - (x^* + c)x^{*2}}{x^{*2} - 2bx^* + b}\tau,$$

then system (2.2) becomes (still denote τ by t)

$$\begin{aligned}\dot{x} &= \widehat{c}_{11}xy + \widehat{c}_{02}y^2 + \widehat{c}_{30}x^3 + \widehat{c}_{21}x^2y + \widehat{c}_{12}xy^2 + \widehat{c}_{03}y^3 + o(|x, y|^3),\\ \dot{y} &= y + \widehat{d}_{20}x^2 + \widehat{d}_{11}xy + \widehat{d}_{02}y^2 + \widehat{d}_{30}x^3 + \widehat{d}_{21}x^2y + \widehat{d}_{12}xy^2 + \widehat{d}_{03}y^3 + o(|x, y|^3),\end{aligned} \tag{2.23}$$

$\widehat{c}_{ij}$ and $\widehat{d}_{ij}$ can be expressed by b, c and x^*, here we omit them for brevity.

According to the center manifold theory, letting $y = \widehat{m}x^2 + \widehat{n}x^3 + o(x^3)$, we can get

$$\widehat{m} = 0, \ \ \widehat{n} = \frac{bc(1-b)(x^{*2} - 2bx^* + b)}{(x^* - b)((c + x^*)x^{*2} - b(3x^{*2} + (2c-3)x^* + 1 - c))^2},$$

then the reduced system restricted to the central manifold is

$$\dot{x} = \frac{bc(1-b)(x^{*2} - 2bx^* + b)}{(x^* - b)((c + x^*)x^{*2} - b(3x^{*2} + (2c-3)x^* + 1 - c))^2}x^3 + O(x^4), \tag{2.24}$$

where the coefficient of x^3-term is not zero since $0 < b < 1$, according to the Theorem 7.1 in chapter 2 of Zhang et al. [40], E^* is an unstable degenerate node of codimension 2 if $b_0 < b < k_2$, and a stable degenerate node of codimension 2 if $b < b_0$.

(II) If $b = b_0$, then the Jacobian matrix of system (2.2) at E^* has two zero eigenvalues. Make the following linear transformations successively:

$$x = X + x^*, \ \ y = Y - \tfrac{x^*(1-x^*)}{c}; \ \ X = x + \tfrac{y}{c}, \ \ Y = x; \ \ x = X, \ \ y = \dot{X},$$

then system (2.2) becomes

$$\begin{aligned}\dot{x} &= y,\\ \dot{y} &= \tilde{a}_{11}xy - \tilde{a}_{30}x^3 - \tilde{a}_{21}x^2y_3 + y^2(\tilde{a}_{02} + \tilde{a}_{12}x + \tilde{a}_{03}y) + o(|x, y|^3),\end{aligned} \tag{2.25}$$

where

$$\begin{aligned}\tilde{a}_{11} &= \frac{c(1-c-2x^*)}{x^*(1-x^*)}, \ \ \tilde{a}_{02} = \frac{1-2x^*}{x^*(1-x^*)}, \ \ \tilde{a}_{30} = \frac{c(c+x^*)(1-c-x^*)}{x^*(1-x^*)(1-c-2x^*)},\\ \tilde{a}_{21} &= -\frac{(c+x^*)(1-c-x^*)(3x^{*2} + (2c-3)x^* + c(c-1))}{x^{*2}(1-x^*)^2(1-c-2x^*)},\\ \tilde{a}_{03} &= -\frac{(c+x^*)^2(1-c-2x^*)^2}{c^2x^{*2}(1-x^*)^2(1-c-2x^*)},\\ \tilde{a}_{12} &= -\frac{2c^4 + 5(2x^*-1)c^3 + (17x^{*2} - 17x^* + 3)c^2 + 5x^*(2x^{*2} - 3x^* + 1)c + 3(1-x^*)^2x^{*2}}{cx^{*2}(1-x^*)^2(1-c-2x^*)},\end{aligned}$$

it is obvious that $\tilde{a}_{30} > 0$ and $\tilde{a}_{21} > 0$ for $0 < x^* < \frac{1-c}{2}$ and $0 < c < 1$.

Next, we make a rescalling of coordinates and time by

$$x = \frac{\sqrt{\tilde{a}_{30}}}{\tilde{a}_{21}}X, \ \ y = \frac{\sqrt{\tilde{a}_{30}^3}}{\tilde{a}_{21}^2}Y, \ \ t = \frac{\tilde{a}_{21}}{\tilde{a}_{30}}\tau,$$

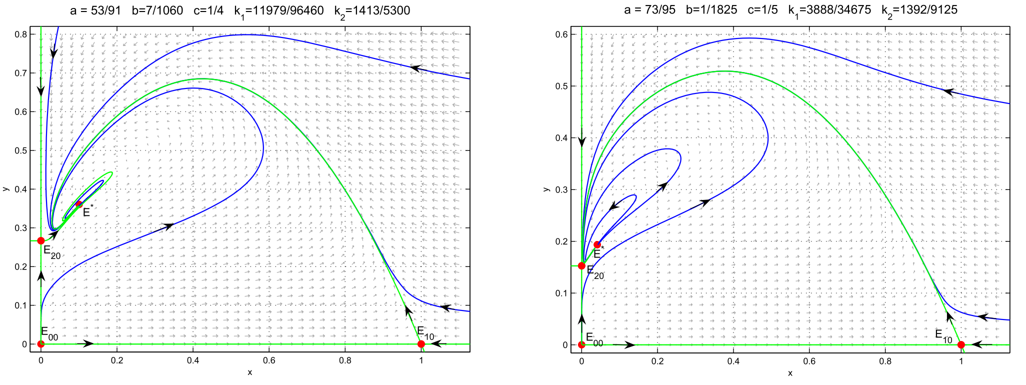

(a) (b)

Fig. 2.3. A unique positive equilibrium E^* of system (1.4) when $b < \min\{1, k_2\}$. (a) A nilpotent focus of codimension 3. (b) A nilpotent elliptic singularity E^* of codimension 3.

then system (2.25) becomes (still denote τ by t)

$$\begin{aligned}\dot{X} &= Y,\\ \dot{Y} &= -X^3 + \tilde{b}_{11}XY - X^2Y + Y(\tilde{b}_{02} + \tilde{b}_{12}X + \tilde{b}_{03}Y) + o(|X, Y|^3),\end{aligned} \tag{2.26}$$

where

$$\tilde{b}_{11} = \frac{\tilde{a}_{11}}{\sqrt{\tilde{a}_{30}}} = \sqrt{\frac{c(1-c-2x^*)^3}{x^*(c+x^*)(1-x^*)(1-c-x^*)}} > 0,$$

$$\tilde{b}_{02} = \frac{\sqrt{\tilde{a}_{30}}\tilde{a}_{02}}{\tilde{a}_{21}}, \quad \tilde{b}_{12} = \frac{\tilde{a}_{30}\tilde{a}_{12}}{\tilde{a}_{21}^2}, \quad \tilde{b}_{03} = \frac{\tilde{a}_{30}^2\tilde{a}_{03}}{\tilde{a}_{21}^3},$$

through a simple calculation, we obtain $\tilde{b}_{11} = 2\sqrt{2}$ is equivalent to $\mathcal{C}(x^*, c) = 0$. Hence, according to [10] (see also [16,24,37]), E^* is a nilpotent focus of codimension 3 if $\mathcal{C}(x^*, c) < 0$, a nilpotent elliptic singularity of codimension 3 (or at least 4) if $\mathcal{C}(x^*, c) > 0$ (or $\mathcal{C}(x^*, c) = 0$). □

Remark 2.8. We next provide some examples to show $\mathcal{C}(x^*, c) < 0$, > 0, $= 0$, respectively.

(1) $\mathcal{C}(x_*, c) = -\frac{95}{256} < 0$ and $(a, b, k_1, k_2) = (\frac{5}{16}, \frac{1}{10}, \frac{3}{80}, \frac{3}{5})$ when $(x_*, c) = (\frac{1}{4}, \frac{1}{4})$, and $E^*(\frac{1}{4}, \frac{3}{4})$ is a nilpotent focus of codimension 3 (Fig. 2.3(a));
(2) $\mathcal{C}(x_*, c) = \frac{7272}{39065} > 0$ and $(a, b, k_1, k_2) = (\frac{73}{95}, \frac{1}{1825}, \frac{3888}{34675}, \frac{1392}{9125})$ for $(x_*, c) = (\frac{1}{25}, \frac{1}{5})$, i.e., $E^*(\frac{1}{25}, \frac{24}{125})$ is a nilpotent elliptic singularity of codimension 3 (Fig. 2.3(b));
(3) $\mathcal{C}(x_*, c) = \frac{7272}{39065} = 0$ and $(a, b, k_1, k_2) = (\frac{50\sqrt{61}-383}{13}, \frac{93\sqrt{61}-721}{596}, \frac{2(45037-5753\sqrt{61})}{1937}, \frac{3091\sqrt{61}-23249}{3576})$ for $(x_*, c) = (\frac{1}{10}(3\sqrt{61}-23), \frac{1}{5}(17-2\sqrt{61}))$, i.e., $E^*(\frac{1}{10}(3\sqrt{61}-23), \frac{5}{24}(7\sqrt{61}-53))$ is a nilpotent elliptic singularity of codimension at least 4.

2.2.2. The case of $b \geq k_2$ (i.e., $q \leq \mu$)

In this case system (1.4) always has three boundary equilibria: hyperbolic unstable node $E_{00}(0,0)$, hyperbolic saddles $E_{10}(1,0)$ and $E_{20}(0,k_2)$. From (2.6), we can see that system (1.4) has exactly one positive equilibrium in $(b,1)$.

Lemma 2.9. *If $k_2 \leq b < 1$ (i.e., $q \leq \mu < \frac{\rho_1}{b_1}$), then system (2.2) (or system (1.4)) has a unique positive equilibrium $E_3(x_3, y_3)$, which is an elementary anti-saddle.*

3. Degenerate Bogdanov-Takens bifurcations of codimension 3

According to Theorems 2.6 and 2.7, we know that system (1.4) may exhibit three types (cusp, focus and elliptic types) of degenerate Bogdanov-Takens bifurcation of codimension 3 by choosing proper bifurcation parameters.

3.1. Cusp case

By Theorem 2.6 we know that system (2.2) may exhibit degenerate Bogdanov-Takens bifurcation of codimension 3 (cusp case) around E_*. To make sure if such a bifurcation can be fully unfolded inside the class of system (2.2), we choose a, k_1 and k_2 as bifurcation parameters, then the unfolding system for system (2.2) takes the following form:

$$\begin{aligned} \dot{x} &= x(1-x) - \frac{(a+\xi_1)(x-b)y}{k_1+\xi_2+x-b}, \\ \dot{y} &= cy\left(1 - \frac{y}{k_2+\xi_3+x-b}\right), \end{aligned} \tag{3.1}$$

where $\xi = (\xi_1, \xi_2, \xi_3) \sim (0,0,0)$.

Theorem 3.1. *When $b < \min\{1, k_2\}$, system (2.2) can undergo a degenerate Bogdanov-Takens bifurcation (cusp case) of codimension 3 around E_* as (a, k_1, k_2) varies near (a_2, k_{12}, k_{22}). There exist a series of bifurcations with codimension 1 and 2 originating from E_*.*

Proof. Following similar steps as in [1,21,37] and performing a sequence of near-identity transformations and time rescaling (preserving orientations of orbits), we can reduce system (3.1) to the following form:

$$\begin{aligned} \dot{x} &= y, \\ \dot{y} &= \eta_1 + \eta_2 y + x^2 + \eta_3 xy - x^3 y + P(x,y,\xi), \end{aligned} \tag{3.2}$$

where $P(x,y,\xi) = y^2 O(|x,y|^2) + O(|x,y|^5) + O(\xi)(O(|y|^2) + O(|x,y|^3)) + O(\xi^2)O(|x,y|)$.

Using MATHEMATICA software we obtain

$$\left|\frac{D(\eta_1,\eta_2,\eta_3)}{D(\xi_1,\xi_2,\xi_3)}\right|_{\xi=0} = \frac{\mathcal{A}_1 \mathcal{M}_1 C_r(x_*,c)}{8x_*^2(1-x_*)^2 \mathcal{A}_2 \sqrt[5]{c^{23}(1-c-2x_*)^{44} C_r(x_*,c)}},$$

where

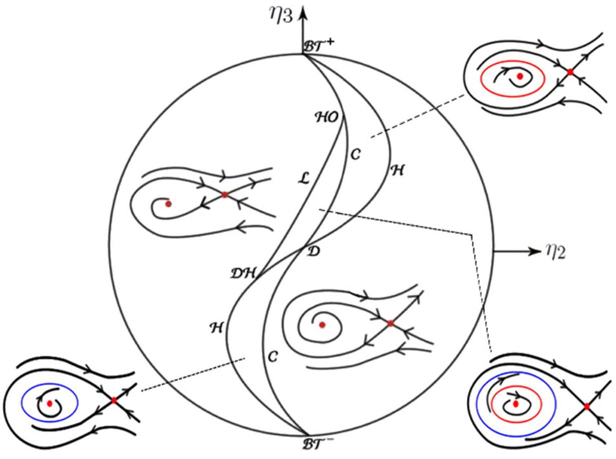

Fig. 3.1. The projection of Bogdanov-Takens bifurcation diagram of codimension 3 (cusp case). $\mathcal{H}, \mathcal{C}, \mathcal{L}, \mathcal{DH}, \mathcal{HO}, \mathcal{D}, \mathcal{BT}$ denote Hopf bifurcation, homoclinic bifurcation, saddle-node bifurcation of limit cycles, degenerate Hopf bifurcation, degenerate homoclinic bifurcation, Hopf and homoclinic bifurcations simultaneously, Bogdanov-Takens bifurcation, respectively.

$$\mathcal{M}_1 = \mathcal{A}_1\mathcal{A}_2 + 4x_*(1-x_*)(1-c^2), \quad \mathcal{A}_1 = 2x_*^2 + 2(c-1)x_* + c(c-1),$$
$$\mathcal{A}_2 = 6x_*^2 + 6(c-1)x_* + c^2 - 3c + 2,$$

and $C_r(x_*, c)$ is given in (2.14). For $x_* \in (\frac{\sqrt{2c(1+c)}-2c}{2}, \frac{1-c}{2})$ and $0 < c < 1$, we can prove $\mathcal{A}_1 < 0$ and $\mathcal{M}_1 > 0$ by using the similar argument as in the proof of Lemma 2.5, for brevity we omit the proof process. Note that $a_2 = -\frac{c\mathcal{A}_2}{\mathcal{A}_1} > 0$ (where a_2 is defined in (2.15)), then $\mathcal{A}_2 > 0$. Moreover, $C_r(x_*, c) < 0$ by Lemma 2.5. Thus we have $\left|\frac{D(\eta_1,\eta_2,\eta_3)}{D(\xi_1,\xi_2,\xi_3)}\right|_{\xi=0} \neq 0$.

According to Dumortier et al. [9], system (3.2) is the versal unfolding of the Bogdanov-Takens singularity (cusp) of codimension 3, and the reminder terms P has no influence on the bifurcation phenomena. Thus the dynamics of system (2.2) (or (1.4)) in a small neighborhood of E_* as (a, k_1, k_2) varying near (a_2, k_{12}, k_{22}) are equivalent to system (3.2) in a small neighborhood of $(0, 0)$ as (μ_1, μ_2, μ_3) varying near $(0, 0, 0)$. □

According to Dumortier et al. [9], we have the projection of Bogdanov-Takens bifurcation diagram of codimension 3 (cusp case) in Fig. 3.1.

Now we summarize the bifurcation phenomena of system (3.2), which is equivalent to those in the original system (2.2). There are three bifurcation curves in Fig. 3.1: $\mathcal{C}$ stands for homoclinic bifurcation curve, $\mathcal{H}$ stands for Hopf bifurcation and $\mathcal{L}$ stands for saddle-node bifurcation curve of limit cycles. The curve $\mathcal{L}$ is tangent to $\mathcal{H}$ at a point $\mathcal{DH}$ and tangent to $\mathcal{C}$ at a point $\mathcal{HO}$. The curves $\mathcal{H}$ and $\mathcal{C}$ have first order contact with boundary of S at the points $\mathcal{BT}^+$ and $\mathcal{BT}^-$. In the neighborhood of $\mathcal{BT}^+$ and $\mathcal{BT}^-$, system (3.2) is an unfolding of the cusp singularity of codimension 2. The detailed bifurcations are listed below:

(1) Codimension-1 bifurcations: Hopf bifurcation $\mathcal{H}$ (except the point $\mathcal{DH}$), homoclinic bifurcation C (except the point $\mathcal{HO}$), saddle-node bifurcation $\mathcal{L}$ of limit cycle;

Table 1
Dynamical behaviors in Fig. 3.2. Here"–", "SN","SF","UF" and "SA" denote"does not exist", "stable node","stable focus", "unstable focus" and"saddle", respectively.

a	k_1	E_2	E_3	Limit cycles and homoclinic orbits
0.6839	0.0413	-	-	No (Fig. 3.2(a))
	0.04147	SA	UF	No (Fig. 3.2(b))
	0.041623	SA	SF	An unstable limit cycle (Fig. 3.2(c))
	0.0416236	SA	SF	An unstable limit cycle, a homoclinic loop (Fig. 3.2(d))
	0.041625	SA	SF	Two limit cycles (inner one unstable) (Fig. 3.2(e))
	0.042	SA	SF	No (Fig. 3.2(f))

(2) Codimension-2 bifurcations: degenerate Hopf bifurcation $\mathcal{DH}$, Bogdanov-Takens bifurcation $\mathcal{BT}^+$ and $\mathcal{BT}^-$, degenerate homoclinic bifurcation $\mathcal{HO}$, Hopf and homoclinic bifurcation simultaneously $\mathcal{D}$.

Next, we provide some numerical simulations to illustrate the theoretical results. Fixing $(b, c, k_2) = (\frac{1}{120}, \frac{1}{2}, \frac{1}{10})$ and varying a and k_1, we plot some phase portraits in Fig. 3.2, where parameter values and corresponding dynamical behaviors are given in Table 1. From Fig. 3.2 and Table 1, we can see that with the increase of k_1, system (2.2) undergoes the following bifurcations successively: saddle-node bifurcation, subcritical Hopf bifurcation, attracting homoclinic bifurcation and saddle-node bifurcation of limit cycles.

3.2. *Focus and elliptic cases*

Define

$$
\begin{aligned}
a_3 &:= \frac{c(3x^{*2} + (2c-3)x^* + 1 - c)}{(c + x^*)(1 - c - x^*)}, \quad b_3 := \frac{x^{*2}(x^* + c)}{3x^{*2} - (3 - 2c)x^* + 1 - c},\\
k_{13} &:= \frac{x^*(1 - x^*)(1 - c - 2x^*)^3}{(c + x^*)(1 - c - x^*)(3x^{*2} + (2c-3)x^* + 1 - c)},\\
k_{23} &:= \frac{x^*(1 - x^*)(3x^{*2} + (4c-3)x^* + (1-c)^2)}{c(3x^{*2} + (2c-3)x^* + 1 - c)},
\end{aligned}
\tag{3.3}
$$

where $0 < x^* < \frac{1-c}{2}$ and $0 < c < 1$.

Theorem 2.7(II) indicates that if $(a, b, k_1, k_2) = (a_3, b_3, k_{13}, k_{23})$ and $\mathcal{C}(x^*, c) \neq 0$, then the unique positive equilibrium E^* of system (2.2) is a nilpotent focus or elliptic singularity of codimension 3, and system (2.2) may exhibit nilpotent focus or elliptic type Bogdanov-Takens bifurcation of codimension 3 around E^*. If we chose a, k_1 and k_2 as bifurcation parameters, then the unfolding system of system (2.2) is

$$
\begin{aligned}
\dot{x} &= x(1 - x) - \frac{(a + \lambda_1)(x - b)y}{k_1 + \lambda_2 + x - b},\\
\dot{y} &= cy\left(1 - \frac{y}{k_2 + \lambda_3 + x - b}\right),
\end{aligned}
\tag{3.4}
$$

where $\lambda = (\lambda_1, \lambda_2, \lambda_3)$ is a parameter vector around $(0, 0, 0)$.

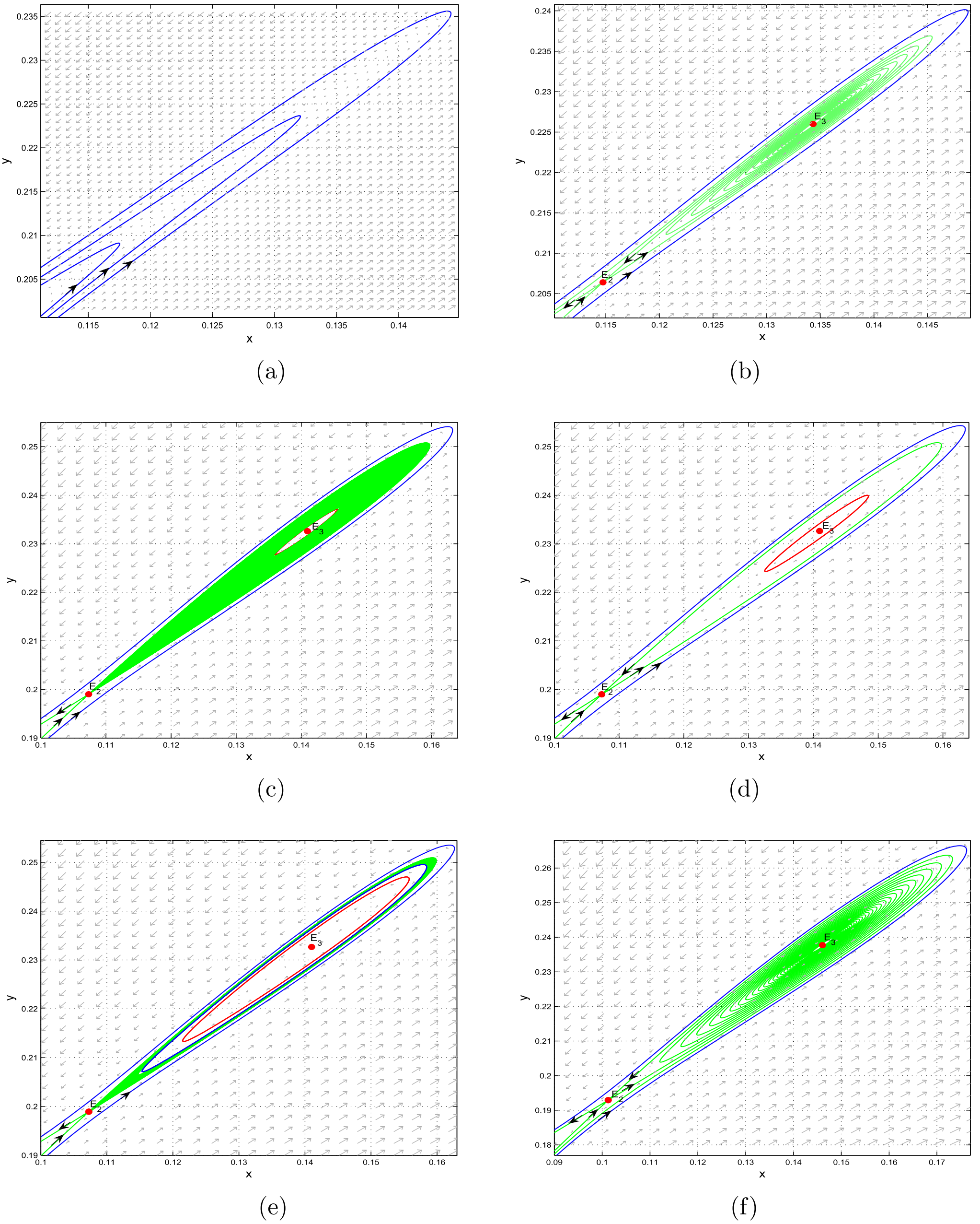

Fig. 3.2. Phase portraits of system (2.2) around nilpotent cusp E_* of codimension 3 with $(a, b, c, k_2) = (\frac{6839}{10000}, \frac{1}{120}, \frac{1}{2}, \frac{1}{10})$. The detailed dynamical behaviors are described in Table 1.

Define

$$\mathcal{G}(x^*, c) = 6x^{*4} - 12(1-2c)x^{*3} + 6(4c^2 - 6c + 1)x^{*2} + 2c(5c^2 - 12c + 7)x^* \\ - c(1-2c)(1-c)^2, \tag{3.5}$$

and

$$\mathcal{R}_+ = \left\{x^* \in (0, \frac{1-c}{2}), c \in (0,1) | \mathcal{G}(x^*, c) > 0\right\}, \\ \mathcal{R}_- = \left\{x^* \in (0, \frac{1-c}{2}), c \in (0,1) | \mathcal{G}(x^*, c) < 0\right\}. \tag{3.6}$$

Remark 3.2. $\mathcal{R}_+$ and $\mathcal{R}_-$ are non-empty. Letting $c = \frac{1}{10}$ and $x^* = \frac{1}{10}$, one has $\mathcal{G}(\frac{1}{10}, \frac{1}{10}) = \frac{1160}{189} > 0$. Letting $c = \frac{1}{10}$ and $x^* = \frac{1}{20}$, one has $\mathcal{G}(\frac{1}{20}, \frac{1}{10}) = \frac{345}{1444} < 0$.

Theorem 3.3. *Suppose $b < \min\{1, k_2\}$, we have*

(I) *if $(x^*, c) \in \mathcal{P}_- \cap \mathcal{R}_+$, then system (2.2) (i.e., system (1.4)) undergoes a degenerate Bogdanov-Takens bifurcation (focus case) of codimension 3 around E^* as (a, k_1, k_2) varies in a small neighborhood of (a_3, k_{13}, k_{23}). There exist a series of bifurcations with codimension 1 and 2 originating from E^*;*

(II) *if $(x^*, c) \in \mathcal{P}_+ \cap \mathcal{R}_+$, then system (2.2) (i.e., system (1.4)) undergoes a degenerate Bogdanov-Takens bifurcation (elliptic case) of codimension 3 around E^* as (a, k_1, k_2) varies in a small neighborhood of (a_3, k_{13}, k_{23}). There exist a series of bifurcations with codimension 1 and 2 originating from E^*.*

Proof. Firstly, we make the following transformations successively

$$x = X + x^*, \quad y = Y + \frac{x^*(1-x_*)}{c};$$

$$X = x + \frac{y}{c}, \quad Y = x;$$

$$x = X + \frac{1-2x^*}{2x^*(1-x^*)}X^2 - \frac{1}{x^*(1-x^*)}XY, \quad y = Y + \frac{1-2x^*}{x^*(1-x^*)}XY,$$

then system (3.4) becomes

$$\dot{X} = Y + \tilde{e}_{00}(\lambda) + \tilde{e}_{10}(\lambda)X + \tilde{e}_{01}(\lambda)Y + \tilde{e}_{20}(\lambda)X^2 + \tilde{e}_{11}(\lambda)XY + +\tilde{e}_{02}(\lambda)Y^2 + \tilde{e}_{30}(\lambda)X^3 \\ + \tilde{e}_{21}(\lambda)X^2Y + \tilde{e}_{12}(\lambda)XY^2 + \tilde{e}_{03}(\lambda)Y^3 + o(|X, Y|^3),$$
$$\dot{Y} = \tilde{f}_{00}(\lambda) + \tilde{f}_{10}(\lambda)X + \tilde{f}_{01}(\lambda)Y + \tilde{f}_{20}(\lambda)X^2 + \tilde{f}_{11}(\lambda)XY + \tilde{f}_{02}(\lambda)Y^2 + \tilde{f}_{30}(\lambda)X^3 \\ + \tilde{f}_{21}(\lambda)X^2Y + \tilde{f}_{12}(\lambda)XY^2 + \tilde{f}_{03}(\lambda)Y^3 + o(|X, Y|^3), \tag{3.7}$$

where $\tilde{e}_{ij}$ and $\tilde{f}_{ij}$ are smooth function of λ_i, c and x^*, to save space we omit the detail expressions. When $\lambda_1 = 0$ $(i = 1, 2, 3)$, we have $\tilde{e}_{00}(0) = \tilde{e}_{10}(0) = \tilde{e}_{01}(0) = \tilde{e}_{20}(0) = \tilde{e}_{11}(0) =$

$\tilde{e}_{02}(0) = \tilde{e}_{30}(0) = \tilde{f}_{00}(0) = \tilde{f}_{10}(0) = \tilde{f}_{01}(0) = \tilde{f}_{20}(0) = \tilde{f}_{02}(0) = 0$, $\tilde{e}_{21}(0) = \tilde{e}_{21}$, $\tilde{e}_{12}(0) = \tilde{e}_{12}$, $\tilde{e}_{03}(0) = \tilde{e}_{03}$, $\tilde{f}_{30}(0) = \tilde{f}_{30}$, $\tilde{f}_{21}(0) = \tilde{f}_{21}$, $\tilde{f}_{12}(0) = \tilde{f}_{12}$, $\tilde{f}_{03}(0) = \tilde{f}_{03}$.

Secondly, we make the following smooth coordinates transformations successively:

$$X = x + \frac{2\tilde{e}_{21}(0) + \tilde{f}_{12}(0)}{6}x^3 + \frac{\tilde{e}_{12}(0) + \tilde{f}_{03}(0)}{2}x^2 y, \ \ Y = y - \frac{\tilde{f}_{12}(0)}{2}x^2 y + \tilde{f}_{03}(0)xy^2 - \tilde{e}_{03}(0)y^3;$$
$$x = X, \ \ y = \frac{dX}{dt},$$

then system (3.7) can be rewritten as

$$\begin{aligned} \dot{x} &= y, \\ \dot{y} &= \tilde{g}_{00}(\lambda) + \tilde{g}_{10}(\lambda)x + \tilde{g}_{01}(\lambda)y + \tilde{g}_{20}(\lambda)x^2 + \tilde{g}_{11}(\lambda)xy + \tilde{g}_{02}(\lambda)y^2 - \tilde{g}_{30}(\lambda)x^3 \\ &\quad - \tilde{g}_{21}(\lambda)x^2 y + \tilde{g}_{12}(\lambda)xy^2 + \tilde{g}_{03}(\lambda)y^3 + o(|x, y|^3), \end{aligned} \tag{3.8}$$

where $\tilde{g}_{ij}(\lambda)$ can be expressed by x^*, c and λ, here we omit them to save space.

Thirdly, notice that

$$\tilde{g}_{30}(0) = \frac{c(c + x^*)(1 - c - x^*)}{x^*(1 - x^*)(1 - c - 2x^*)} > 0, \ \ \tilde{g}_{21}(0) = \frac{\mathcal{G}(x^*, c)}{2[x^*(1 - x^*)]^2(1 - c - 2x^*)},$$

obviously, $2[x^*(1 - x^*)]^2(1 - c - 2x^*) > 0$ since $0 < x^* < \frac{1-c}{2}$. Thus $\tilde{g}_{21}(0) > 0$ when $(x^*, c) \in \mathcal{P}_- \cap \mathcal{R}_+$. Next, we first analyze the case $\tilde{g}_{21}(0) > 0$ (the case $\tilde{g}_{21}(0) < 0$ can be treated similarly), making the following smooth coordinate transformations successively:

$$x = X - \frac{\tilde{g}_{20}(\lambda)}{3\tilde{g}_{30}(\lambda)}, \ \ y = Y;$$
$$X = \frac{\sqrt{\tilde{g}_{30}(\lambda)}}{\tilde{g}_{21}(\lambda)}x, \ \ Y = \frac{\sqrt{\tilde{g}_{30}^3(\lambda)}}{\tilde{g}_{21}^2(\lambda)}y, \ \ t = \frac{\tilde{g}_{21}(\lambda)}{\tilde{g}_{30}(\lambda)}\tau, \tag{3.9}$$

then system (3.9) becomes (still denote τ by t)

$$\begin{aligned} \dot{x} &= y, \\ \dot{y} &= \varepsilon_1(\lambda) + \varepsilon_2(\lambda)x - x^3 + y[\varepsilon_3(\lambda) + A_1(\lambda)x - x^2] + y^2 Q(x, y, \lambda) + o(|x, y|^3), \end{aligned} \tag{3.10}$$

where $\varepsilon_i(\lambda)$ $(i = 1, 2, 3)$ and $A_1(\lambda)$ can be expressed by λ_i $(i = 1, 2, 3)$, x^* and c, $Q(x, y, \lambda)$ is a C^∞ function at most first order with respect to (x, y), whose coefficients depend smoothly on λ_1, λ_2 and λ_3, we omit the detail expressions here to save space.

Since

$$\left| \frac{\partial(\varepsilon_1, \varepsilon_2, \varepsilon_3)}{\partial(\lambda_1, \lambda_2, \lambda_3)} \right|_{\lambda=0} = \frac{cx^*(1 - x^*)\mathcal{G}_2(x^*, c)\tilde{g}_{21}^6(0)}{3\sqrt{\tilde{g}_{30}^7(0)}\mathcal{G}_3(x^*, c)},$$

where

$$\mathcal{G}_2(x^*, c) = 3x^{*2} + (4c-3)x^* + 2c(c-1), \;\; \mathcal{G}_3(x^*, c) = 3x^{*2} + (2c-3)x^* + 1 - c,$$

treating x^* as variable in $\mathcal{G}_2(x^*, c)$ and $\mathcal{G}_3(x^*, c)$, we can get $\mathcal{G}_2(x^*, c) < \max\{\mathcal{G}_2(\frac{1-c}{2}, c), \mathcal{G}_2(0, c)\} = \max\left\{\frac{3(c^2-1)}{4}, 2c(c-1)\right\} < 0$ and $\mathcal{G}_3(x^*, c) > \mathcal{G}_2(\frac{1-c}{2}, c) = \frac{1-c^2}{4} > 0$ for any $c \in (0, 1)$. Hence, if $(x^*, c) \in \mathcal{R}_\pm$, then $\left|\frac{\partial(\varepsilon_1,\varepsilon_2,\varepsilon_3)}{\partial(\lambda_1,\lambda_2,\lambda_3)}\right|_{\lambda=0} \neq 0$. Furthermore, in system (3.10), the coefficients of x^3 and x^2y are -1, the coefficient of xy is $A_1(\lambda)$, and

$$0 < A_1(0) = \frac{\tilde{g}_{11}(0)}{\sqrt{\tilde{g}_{30}(0)}} = \sqrt{\frac{c(1-c-2x^*)^3}{x^*(c+x^*)(1-x^*)(1-c-x^*)}},$$

further analysis shows that system (3.10) is a generic 3-parameter family of nilpotent focus of codimension 3 if $(x^*, c) \in \mathcal{P}_- \cap \mathcal{R}_+$; a generic 3-parameter family of nilpotent elliptic singularity of codimension 3 if $(x^*, c) \in \mathcal{P}_+ \cap \mathcal{R}_+$ [10]. □

Remark 3.4. $\mathcal{P}_- \cap \mathcal{R}_+$ and $\mathcal{P}_+ \cap \mathcal{R}_+$ are non-empty. If $(x^*, c) = (\frac{1}{10}, \frac{1}{4})$, then $\tilde{g}_{21}(0) = \frac{16655}{1188} > 0$, and $A_1(0) = \frac{11\sqrt{55}}{6\sqrt{91}} < 2\sqrt{2}$, hence, $\mathcal{P}_- \cap \mathcal{R}_+$ is non-empty. If $(x^*, c) = (\frac{1}{20}, \frac{1}{4})$, then $\tilde{g}_{21}(0) = \frac{5487025}{823296} > 0$, and $A_1(0) = \frac{335\sqrt{67}}{8\sqrt{12354}} > 2\sqrt{2}$, hence, $\mathcal{P}_+ \cap \mathcal{R}_+$ is non-empty.

According to Dumortier et al. [10], we have the bifurcation diagram (focus case) in Fig. 3.3. From Fig. 3.3, we can see that there exist a series of bifurcations with codimension 1 and 2 originating from the nilpotent focus E^* of codimension 3, such as:

- **(I)** Codimension-1 bifurcations: a Hopf bifurcation, three homoclinic bifurcations, two saddle-node homoclinic bifurcations, a saddle-node bifurcation of limit cycles and two saddle-node bifurcations;
- **(II)** Codimension-2 bifurcations: a degenerate Hopf bifurcation, two Bogdanov-Takens bifurcations, two cuspidal bifurcations, a degenerate homoclinic bifurcation and four saddle-node homoclinic bifurcations.

Next, we provide some numerical phase portraits to illustrate the theoretical results. Fixing $(b, c, k_2) = (\frac{7}{1060}, \frac{1}{4}, \frac{4}{25})$, we plot some typical phase portraits in Fig. 3.4, where the parameter values and corresponding dynamical behaviors are given in Table 2. From Fig. 3.4 and Table 2, we can see that system (2.2), as a and k_1 vary, can undergo following bifurcations: saddle-node bifurcation (Fig. 3.4(a)(d)), supercritical Hopf bifurcation (Fig. 3.4(a)(b)), subcritical Hopf bifurcation (Fig. 3.4(b)(c)), Degenerate Hopf bifurcation of codimension 2 (Fig. 3.4 (a)(c)).

4. Hopf bifurcation of codimension 3

From Lemma 2.3 or Lemma 2.9, we know that E_1 or E_3 is an elementary anti-saddle, which can be a center-type equilibrium if $\mathrm{Tr}(J(E_1)) = 0$ or $\mathrm{Tr}(J(E_3)) = 0$, and system (1.4) may exhibit Hopf bifurcation around E_1 or E_3. For simplification, we use z to denote x_i $(i = 1, 3)$ and E_z to denote the equilibrium $(z, \frac{z(1-z)}{a+c+2z-1})$.

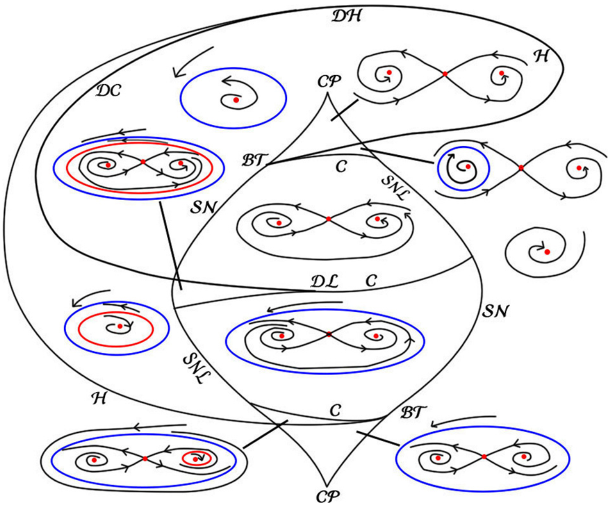

Fig. 3.3. The projection of Bogdanov-Takens bifurcation diagram of codimension 3 (focus case). $\mathcal{H}, \mathcal{C}, \mathcal{SN}, \mathcal{DH}, \mathcal{CP}, \mathcal{BT}, \mathcal{DC}, \mathcal{DL}, \mathcal{SNL}$ denote Hopf bifurcation, Homoclinic bifurcation, saddle-node bifurcation, degenerate Hopf bifurcation point, cuspidal point of codimension 2, Bogdanov-Takens bifurcation point, saddle-node bifurcation of limit cycle, Homoclinic to neutral saddle, Homoclinic to saddle-node, respectively.

Table 2
Dynamical behaviours in Fig. 3.4 with $(b, c, k_2) = (\frac{7}{1060}, \frac{1}{4}, \frac{4}{25})$.

(a, k_1)	E_1	E_2	E_3	Limit cycle and homoclinic loop
(0.6, 0.085)	-	-	SF	No (Fig. 3.4(a))
(0.6, 0.075)	-	-	UF	A stable limit cycle (Fig. 3.4(b))
(0.55, 0.063)	-	-	SF	Two limit cycles (inner one stable) (Fig. 3.4(c))
(0.5, 0.045)	SF	SA	SF	No (Fig. 3.4(d))
(0.52, 0.048)	SF	SA	SF	An unstable limit cycle (Fig. 3.4(e))
(0.55, 0.052)	SF	SA	UF	No (Fig. 3.4(f))
(0.65, 0.0776)	SF	SA	UF	A big stable limit cycle (Fig. 3.4(g))
(0.65, 0.0778)	SF	SA	UF	Two limit cycles (one small encircle E_1) (Fig. 3.4(h))
(0.652, 0.0783)	UF	SA	UF	A big stable limit cycle (Fig. 3.4(i))

Make a time variation $t = \frac{\tau}{(k_1+x-b)(k_2+x-b)}$, then system (2.2) becomes (still denote τ by t)

$$\begin{aligned} \dot{x} &= (k_2 + x - b)(x(1-x)(k_1 + x - b) - a(x-b)y), \\ \dot{y} &= c(k_1 + x - b)y(k_2 + x - b - y). \end{aligned} \tag{4.1}$$

From $\mathrm{Tr}(J(E_z)) = F(z) = 0$, we have

$$a^H := \frac{z^2(1-z)^2}{(k_2 + z - b)(z(c+z) + b(1-c-2z))}, \quad k_1^H := \frac{(z-b)^2(1-c-2z)}{z(c+z) + b(1-c-2z)}. \tag{4.2}$$

By simple calculation, we can claim that $a^H > 0$, $k_1^H > 0$ and $\mathrm{Det}(J(E_z)) > 0$ if and only if $(b, c, k_2, z) \in \mathcal{D}$, where

$$\mathcal{D} := \left\{ (b, c, k_2, z) \in \mathbb{R}_+^4 | 0 < b < z, 0 < c < 1, 0 < k_2 < \tfrac{(1-c-z)z+bc}{c}, 0 < z < \tfrac{1-c}{2} \right\}. \tag{4.3}$$

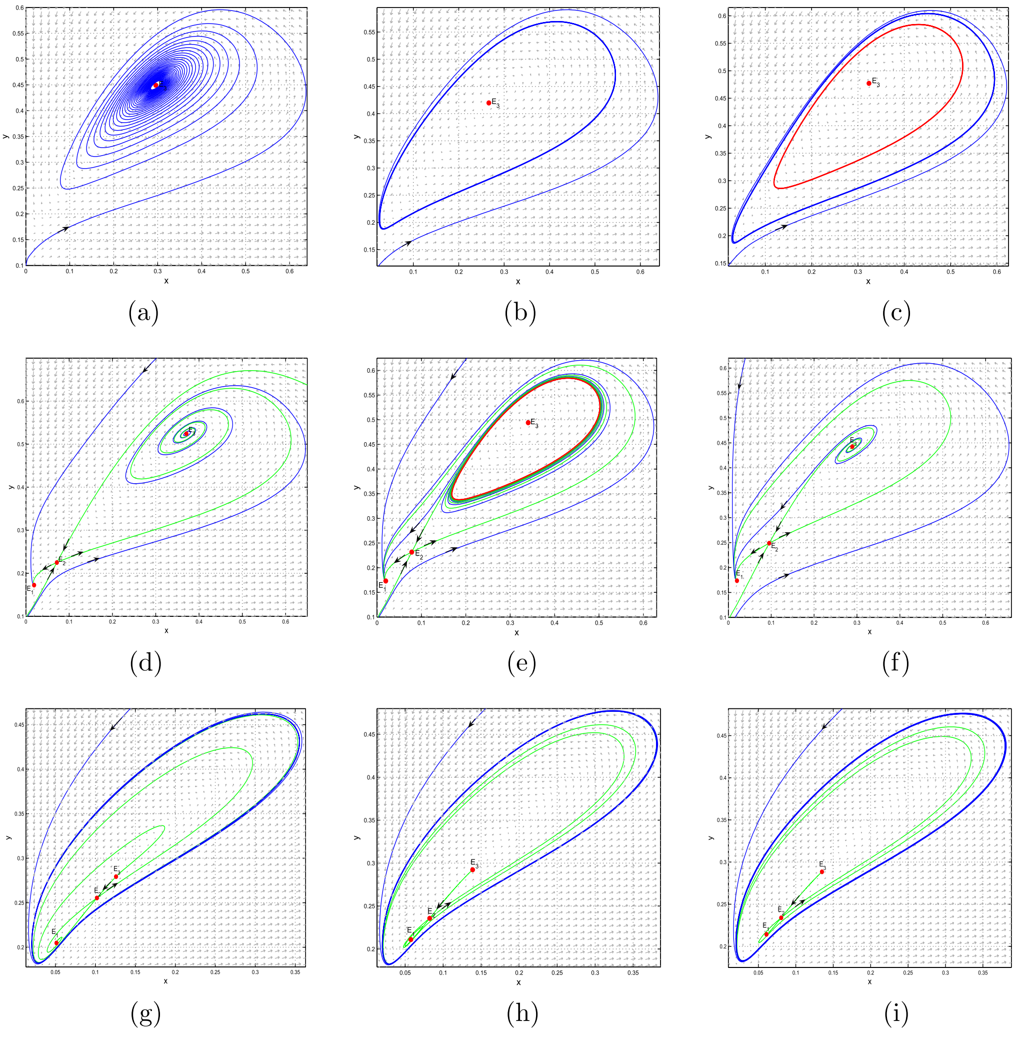

Fig. 3.4. Phase portraits of system (3.4) around nilpotent focus E^* of codimension 3 with $(b, c, k_2) = (\frac{7}{1060}, \frac{1}{4}, \frac{4}{25})$. The detailed dynamical behaviors are described in Table 2.

Next, by a sequence of coordinates transformations and formal series method [40], we obtain the first two Lyapunov numbers as follows

$$L_1 = \frac{(z-b)z^2(1-z)^2 g_1}{(z(c+z)+b(1-c-2z))^3 d_1^{\frac{3}{2}}},$$

$$L_2 = \frac{g_2}{(z(c+z)+b(1-c-2z))z^2(1-z)^2c^3(z-b)^3((1-z)z-(k_2+z-b)c)^3(k_2+z-b)^4 d_1^{\frac{1}{2}}}, \tag{4.4}$$

where

$$d_1 = \frac{c(k_2+z-b)((1-z)z-(k_2+z-b)c)z^2(1-z)^2(z-b)^2}{(z(c+z)+b(1-c-2z))^2},$$

g_1 is given in Appendix B, while the expression of g_2 is too long, so we omit it.

Owing to the complexity of L_1 and L_2, here we use the following three specific cases to explore the sign of L_i $(i=1,2)$. Let

$$\begin{aligned}
&(b^{1h}, c^{1h}, k_2^{1h}, z^{1h}) := (\frac{1}{10}, \frac{1}{5}, \frac{1}{5}, \frac{1}{4}), \quad (b^{2h}, c^{2h}, k_2^{2h}, z^{2h}) := (\frac{1}{20}, \frac{1}{4}, \frac{1}{2}, \frac{1}{4}),\\
&(b^{3h}, c^{3h}, k_2^{3h}, z^{3h}) := (\frac{1}{10}, \frac{1}{5}, \frac{73+\sqrt{7849}}{360}, \frac{1}{5}),
\end{aligned} \tag{4.5}$$

which satisfy $(b,c,k_2,z) \in \mathcal{D}$ and the Jacobian matrix $J(E_z)$ has a pair of pure imaginary eigenvalues. Substituting (4.5) into (4.4), we have

$$\begin{aligned}
&L_1|_{(b,c,k_2,z)=(b^{1h},c^{1h},k_2^{1h},z^{1h})} = -\frac{1091576\sqrt{3}}{329\sqrt{329}} < 0, \quad L_1|_{(b,c,k_2,z)=(b^{2h},c^{2h},k_2^{2h},z^{2h})} = \frac{1625}{7\sqrt{14}} > 0,\\
&L_1|_{(b,c,k_2,z)=(b^{3h},c^{3h},k_2^{3h},z^{3h})} = 0, \quad L_2|_{(b,c,k_2,z)=(b^{3h},c^{3h},k_2^{3h},z^{3h})} \doteq -115482.9,
\end{aligned} \tag{4.6}$$

and

$$\begin{aligned}
&\frac{\partial \mathrm{Tr(J(E_z))}}{\partial a}|_{(a,b,c,k_1,k_2,z)=(a^H,b^{1h},c^{1h},k_1^H,k_2^{1h},z^{1h})} = -\frac{7}{40},\\
&\frac{\partial \mathrm{Tr(J(E_z))}}{\partial a}|_{(a,b,c,k_1,k_2,z)=(a^H,b^{2h},c^{2h},k_1^H,k_2^{1h},z^{2h})} = -\frac{63}{100},\\
&\frac{\partial (\mathrm{Tr(J(E_z))},\ \mathrm{L_1})}{\partial (a,k_2)}|_{(a,b,c,k_1,k_2,z)=(a^H,b^{3h},c^{3h},k_2^{3h},k_1^H,z^{3h})} \doteq -1233.17,
\end{aligned}$$

which implies system (2.2) (or system (1.4)) can undergo supercritical Hopf bifurcation, subcritical Hopf bifurcation (Fig. 4.1) and degenerate Hopf bifurcation.

Next we give another example to explore the existence of Hopf bifurcation of codimension 3. Define

$$\begin{aligned}
&\mathcal{D}_1 := \{(b,c,k_2,z) \in \mathcal{D} | L_1 \neq 0\},\\
&\mathcal{D}_2 := \{(b,c,k_2,z) \in \mathcal{D} | L_1 = 0, L_2 \neq 0\},\\
&\mathcal{D}_3 := \{(b,c,k_2,z) \in \mathcal{D} | L_1 = 0, L_2 = 0\}.
\end{aligned} \tag{4.7}$$

Theorem 4.1. *If $(b,c,k_2,z) \in \mathcal{D}$, then system (2.2)(or system (1.4)) has a weak focus E_z. Moreover,*

(1) *E_z is a weak focus of order 1, if $(b,c,k_2,z) \in \mathcal{D}_1$;*
(2) *E_z is a weak focus of order 2, if $(b,c,k_2,z) \in \mathcal{D}_2$;*
(3) *E_z is a weak focus of order at least 3, if $(b,c,k_2,z) \in \mathcal{D}_3$.*

By (4.6), we know that the sets $\mathcal{D}_1$ and $\mathcal{D}_2$ are nonempty. Next, we give an example to show that D_2 is also nonempty, i.e., E_z can be a weak focus of order 3 and system (2.2) can undergo degenerate Hopf bifurcation of codimension 3 near E_z.

Theorem 4.2. *If* $(a, b, c, k_1, k_2, z) = (a^H, -\frac{\chi_1(z)}{\chi_2(z)}, \frac{1}{4}, k^H, k^H, \bar{z})$*, then* E_z *is a weak focus of order 3 and system* (1.4) *can undergo a degenerate Hopf bifurcation of codimension 3 near* E_z*. Where* a^H *and* k^H *are given in* (4.8)*,* $\chi_1(z)$ *and* $\chi_2(z)$ *are given in Appendix D,* $\bar{z}$ *is the unique real root of* $8192z^6 - 18432z^5 + 13056z^4 - 1952z^3 - 1152z^2 + 400z - 7 = 0$ *in the interval* $(0, \frac{3}{8})$.

Proof. Let $k_1 = k_2$, again by $\mathrm{Tr}(J(E_z)) = F(z) = 0$, we have

$$a = a^H := \frac{z(1-z)}{z-b}, \quad k = k^H := \frac{(z-b)^2(1-c-2z)}{z(c+z)+b(1-c-2z)}. \tag{4.8}$$

Fix $c = \frac{1}{4}$. From $a^H > 0$, $k^H > 0$ and $\mathrm{Det}(J(E_z)) > 0$, we have $(b, z) \in \mathcal{D}^*$, where

$$\mathcal{D}^* := \left\{(b, z) \in \mathbb{R}_+^2 | 0 < b < z, 0 < z < \tfrac{3}{8}\right\}. \tag{4.9}$$

Through a series of time and variable transformations, with the aid of MAPLE software, we obtain the first three Lyapunov numbers

$$\begin{aligned}
\bar{L}_1 &= \frac{\bar{g}_1}{32z(1-z)(z^2-2bz+b)(z-b)^2\sqrt{d_2}},\\
\bar{L}_2 &= \frac{\bar{g}_2}{2048z^3(1-z)^3(z^2-2bz+b)^3(z-b)^5\sqrt{d_2}},\\
\bar{L}_3 &= \frac{\bar{g}_3}{131072z^5(1-z)^5(z^2-2bz+b)^5(z-b)^8\sqrt{d_2}},
\end{aligned} \tag{4.10}$$

where

$$\begin{aligned}
d_2 &= \frac{z^2(1-z)^2(z^3-3bz^2+b(1+2b)z-b^2)}{(4z^2+(1-8b)z+3b)^2},\\
\bar{g}_1 &= -3(640z^4-1088z^3+692z^2-190z+21)b^3\\
&\quad +(3072z^4-3696z^3+1412z^2-119z+6)zb^2\\
&\quad -(1536z^4-864z^3-164z^2+176z-9)z^2b+(256z^3-28z-3)z^4,
\end{aligned}$$

$\bar{g}_2$ is given in Appendix C, and the expression of $\bar{g}_3$ is too long, we omit it to save space.

Let the algebraic variety $V(p_1, p_2, \ldots, p_n)$ denote the set of common zeros of p_i $(i = 1, 2, \ldots, n)$, $\mathrm{res}(f, g, x)$ denotes the Sylvester resultant of f and g with respect to x, $\mathrm{lcoeff}(f, x)$ denotes the leading coefficient of the polynomial f with respect to x, and $\mathrm{prem}(f, g, x)$ denotes the pseudoremainder of f with respect to g in x.

Notice that the denominators of $\bar{L}_i$ are nonzero if $(b, z) \in \mathcal{D}^*$, then we have

$$V(\bar{L}_1, \bar{L}_2, \bar{L}_3) \cap \mathcal{D}^* = V(\bar{g}_1, \bar{g}_2, \bar{g}_3) \cap \mathcal{D}^*.$$

Next we prove that $V(\bar{g}_1, \bar{g}_2, \bar{g}_3) \cap \mathcal{D}^* = \emptyset$, i.e., $\bar{L}_i$ $(i = 1, 2, 3)$ have no common zero in $\mathcal{D}^*$, and E_z is a weak focus of order at most 3 for $(b, c) \in \mathcal{D}^*$.

By a straightforward calculation, we have $\mathrm{lcoeff}(\bar{g}_1, b) = -3(640z^4 - 1088z^3 + 692z^2 - 190z + 21) < 0$, for $z \in (0, \frac{3}{8})$. Using MAPLE command "resultant", we have

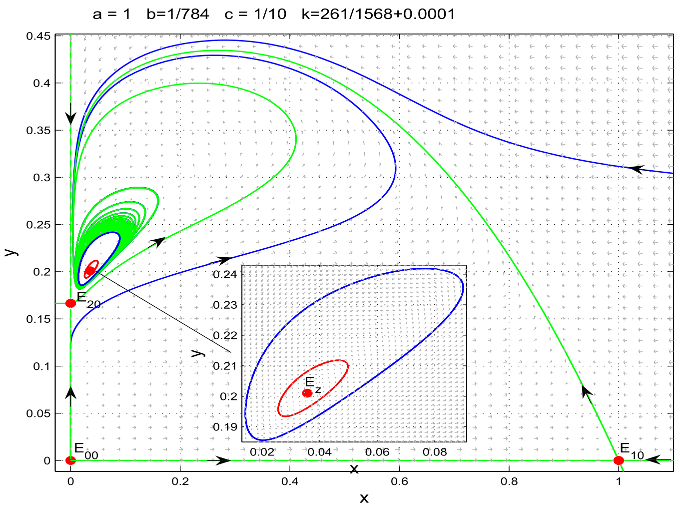

Fig. 4.1. Two limit cycles (outer one is stable).

$$
\begin{aligned}
r_{12} &:= \operatorname{res}(\bar{g}_1, \bar{g}_2, b) = -2334666046828865126 40(1+8z)(7-8z)(3-4z)^2(1+4z)^2(3-8z)^5 \\
&\quad z^{31}(1-z)^{31}\mathcal{R}_1^2\mathcal{R}_2 \\
r_{13} &:= \operatorname{res}(\bar{g}_1, \bar{g}_3, b) = 6016388590926948136009743728640(1+8z)(7-8z)(3-4z)^2(1+4z)^2 \\
&\quad (3-8z)^5 z^{49}(1-z)^4 9\mathcal{R}_1^2\mathcal{R}_3,
\end{aligned}
\tag{4.11}
$$

where

$$
\begin{aligned}
\mathcal{R}_1 &= 32z^2 - 40z + 3, \quad \mathcal{R}_2 = 8192z^6 - 18432z^5 + 13056z^4 - 1952z^3 - 1152z^2 + 400z - 7, \\
\mathcal{R}_3 &= 463352847662013480960 00z^{23} - 4772381912218850033664 00z^{22} + 2244912193045140 0 \\
&\quad 99563520z^{21} - 636703422381263489807155 2z^{20} + 120889502596914899205488 64z^{19} - \\
&\quad 160875072838394711742873 60z^{18} + 151808883880750423526604 80z^{17} - 990221639440 \\
&\quad 8106339074048z^{16} + 398893651659630550450176 0z^{15} - 465646406458420662108160z^{14} \\
&\quad - 509484700433378100379648z^{13} + 342692059064621484998656z^{12} - 87117366831686 \\
&\quad 959497216z^{11} - 29922515375663962193 92z^{10} + 8800364680459792224256z^9 - 2521601 \\
&\quad 568729688381440z^8 + 197402623249857128448z^7 + 6562940969761456819 2z^6 - 226963 \\
&\quad 22247537700896z^5 + 3251291444861229360z^4 - 240018936152525532z^3 + 78773823795 \\
&\quad 98511z^2 - 42697872914553z - 732926685600.
\end{aligned}
$$

Notice that the common factors of r_{12} and r_{13} are nonzero for $0 < z < \frac{3}{8}$, then according to Lemma 1 in [8], we have the following decomposition:

$$V(\bar{g}_1, \bar{g}_2, \bar{g}_3) = V(\bar{g}_1, \bar{g}_2, \bar{g}_3, \mathrm{lcoeff}(\bar{g}_1, b)) \cup V\left(\frac{\bar{g}_1, \bar{g}_2, \bar{g}_3, r_{12}, r_{13}, \mathrm{lcoeff}(r_{12}, z)}{\mathrm{lcoeff}(\bar{g}_1, b)}\right)$$
$$\cup V\left(\frac{\bar{g}_1, \bar{g}_2, \bar{g}_3, r_{12}, r_{13}, \mathrm{res}(r_{12}, r_{13}, z)}{\mathrm{lcoeff}(r_{12}, z), \mathrm{lcoeff}(\bar{g}_1, b)}\right). \tag{4.12}$$

$\mathrm{res}(r_{12}, r_{13}, z) = 0$ since r_{12} and r_{13} have common factors.

Again by Lemma 1 in [8], we have

$$V(r_{12}, r_{13}) = V(\mathcal{R}_1) \cup V(\mathcal{R}_2, \mathcal{R}_3),$$

and note that $\mathrm{lcoeff}(r_{12}, z) = 105144011385330259477742550666706944 0 \neq 0$, then the decomposition (4.12) can be simplified as

$$V(\bar{g}_1, \bar{g}_2, \bar{g}_3) \cap \mathcal{D}^* = V_1 \cup V_2,$$

where

$$\begin{aligned} V_1 &:= V(\bar{g}_1, \bar{g}_2, \bar{g}_3, \mathcal{R}_1) \cap \mathcal{D}^*, \\ V_2 &:= V(\bar{g}_1, \bar{g}_2, \bar{g}_3, \mathcal{R}_2, \mathcal{R}_3) \cap \mathcal{D}^*. \end{aligned}$$

Next, we use two steps to illustrate $V(\bar{g}_1, \bar{g}_2, \bar{g}_3) \cap \mathcal{D}^* = \emptyset$.

Step 1. Proving that $V_1 = \emptyset$. From $\mathcal{R}_1 = 0$, we have

$$z_1 := \tfrac{5-\sqrt{19}}{8} < \tfrac{3}{8}. \tag{4.13}$$

Substituting $z = z_1$ into $\bar{L}_1$ leads to

$$\bar{L}_{11} = \frac{64\bar{g}_{11}}{(8(\sqrt{19}-1)b + 22 - 5\sqrt{19})(8(\sqrt{19}-2)b + 29 - 7\sqrt{19})^2\sqrt{d_3}} \tag{4.14}$$

where

$$\begin{aligned} \bar{g}_{11} &= 2304(59\sqrt{19} - 283)b^3 + 160(12248 - 2809\sqrt{19})b^2 - 8(256828 - 58919\sqrt{19})b \\ &\quad + 717531 - 164613\sqrt{19}, \\ d_3 &= \frac{64(1-\sqrt{19})b^2 - 8(46 - 11\sqrt{19})b + 205 - 47\sqrt{19}}{(8(\sqrt{19}-2)b + 27 - 6\sqrt{19})^2}, \end{aligned}$$

by a simple calculation, here we claim that $\bar{L}_{11} < 0$ for any $b \in (0, z_1)$, which implies $V(\bar{g}_1, \mathcal{R}_1) \cap \mathcal{D}^* = \emptyset$. Hence, $V_1 = \emptyset$.

Step 2. Proving that $V_2 = \emptyset$. Using "resultant" command in MAPLE again, we have

$$\begin{aligned} \mathrm{res}(\mathcal{R}_2, \mathcal{R}_3, z) = {} & 13631755285371842411362879740097999721118045706215253931674892352 9 \\ & 40784738914485736396853691869346547905801462320341625935543995059 \\ & 10061056692209447243528273920000000092209447243528273920000000 0, \end{aligned}$$

then $V(\mathcal{R}_2, \mathcal{R}_3) = \emptyset$, that is $V_2 = \emptyset$.

Next, we will prove that E_z can be a weak focus of order exactly 3 if $c = \frac{1}{4}$ and $\mathcal{R}_2 = 0$. By the MAPLE command "realroot($\mathcal{R}_2$, $1/10^6$)" to isolate the real roots of $\mathcal{R}_2$, we see that $\mathcal{R}_2$ has a unique real zero $\bar{z} \doteq 0.018514456 \in (0, \frac{3}{8})$, which covered by

$$I = \left[\frac{1366125727704958131}{7378697629483820646}, \frac{5464502910819832551}{29514790517935282585}\right] \subseteq (0, \frac{3}{8}).$$

To find the dependence of b on z, we employ the Maple command "prem" to get

$$\begin{aligned} w_1 &:= \text{prem}(\bar{g}_2, \bar{g}_1, b) = 6144(3-8z)z^7(1-z)^7 w_{11}, \\ w_2 &:= \text{prem}(\bar{g}_1, w_1, b) = 7044820107264(3-8z)^3 w_{21}^6 z^{18}(1-z)^{18}(\chi_1(z) + \chi_2(z)b), \end{aligned} \tag{4.15}$$

where

$$w_{21} = 640z^4 - 1088z^3 + 692z^2 - 190z + 21,$$

w_{11}, $\chi_1(z)$ and $\chi_2(z)$ are given in Appendix D. Following the same logic in the proof Lemma 2.5, we obtain that $\text{lcoeff}(w_1, b) > 0$ for $z \in I$, where

$$\text{lcoeff}(w_1, b) = 6144(3-8z)z^7(1-z)^7 w_{12}, \tag{4.16}$$

and w_{12} is given in Appendix D.

From a pseudo-remainder formula in [19], $\text{lcoeff}(\bar{g}_1, b) < 0$ and $\text{lcoeff}(w_1, a) > 0$, we can deduce that $\bar{g}_1 = \bar{g}_2 = 0$ if and only if $w_1 = w_2 = 0$. Moreover, according to Sturm's Theorem, we have $\chi_2(z) \neq 0$ for all $z \in I$, thus, from $w_2 = 0$, b can be solved as

$$b = \bar{b} := -\frac{\chi_1(z)}{\chi_2(z)}.$$

Using Sturm's Theorem again, we obtain that the derivative $(-\frac{\chi_1(z)}{\chi_2(z)})' > 0$ for all $z \in I$. Therefore the function $-\frac{\chi_1(z)}{\chi_2(z)}$ is strictly increasing in I, and it can be easily checked that

$$0.0002062863407 < b < 0.0002062863408 < z, \quad \text{for } z \in I.$$

Therefore,

$$V(\bar{L}_1, \bar{L}_2) \cap \mathcal{D}^* = V(\bar{g}_1, \bar{g}_2, r_{12}) \cap \mathcal{D}^* \neq \emptyset.$$

Finally, by MATHEMATICA we have

$$\left|\frac{\partial(\text{Tr}(E_z), \bar{L}_1, \bar{L}_2)}{\partial(b, c, z)}\right|_{(a,k,c)=(a^H, k^H, \frac{1}{4})} = \frac{J_1(b,z)}{65536(z^2 - 2bz + b)^6 z^7 (1-z)^7 (z-b)^9},$$

here the expression of $J_1(b, z)$ is omitted to save space. By a simple calculation, we know that $(z^2 - 2bz + b)^6 z^7 (1-z)^7 (z-b)^9 > 0$ for $(b, z) \in \mathcal{D}^*$. Using MAPLE again one can easily get

$$\mathrm{res}(\mathcal{R}_2, J_1(b,z), z) = 6556419088368003203611501172158618282758242304000000000 J_2(b)$$

where $J_2(b)$ is a polynomial in b of degree 90, we omit it for brevity. Using MAPLE command "realroot($J_2(b)$, $1/10^6$)", we have $J_2(b) \neq 0$ for $b \in (0.0002062, 0.0002063)$. Hence $\left|\frac{\partial(\mathrm{Tr}(E_z), \bar{L}_1, \bar{L}_2)}{\partial(b,c,z)}\right| \neq 0$ for $(b,c,z) = (\bar{b}, \frac{1}{4}, \bar{z})$. Thus, system (1.4) can undergo a degenerate Hopf bifurcation of codimension 3 near E_z, if $(a,b,c,k_1,k_2,z) = (a^H, -\frac{\chi_1(z)}{\chi_2(z)}, \frac{1}{4}, k^H, k^H, \bar{z})$. □

5. Concluding remarks

In this paper, we revisited a Holling-Tanner model with generalist predator and constant prey refuge. We discussed the impact of the constant prey refuge on the dynamics and bifurcations, and found that the constant prey refuge can induce much richer dynamical behaviors and bifurcation phenomena, such as three types of degenerate Bogdanov-Takens bifurcation of codimension 3 (cusp, focus and elliptic cases) and Hopf bifurcation of codimension at least 3. Numerical simulations, including bifurcation diagrams and phase portraits, are provided to illustrate and complement our analytical results.

We showed that the parameter b (i.e., the constant prey refuge μ) can have an essential effect on not only the number and types of boundary and positive equilibria (see Lemmas 2.1, 2.3, 2.9, and Theorems 2.4, 2.6, 2.7, 4.1), but also the types and codimension of bifurcations (see Theorems 3.1, 3.3, 4.2).

Compared the results in system (1.4) with those in system (1.2), we observe that constant prey refuges can induce more complex dynamical behaviors and bifurcation phenomena. For system (1.2), Xiang *et al.* [38] showed the existence of at most two positive equilibria, only one type of degenerate Bogdanov-Takens bifurcation of codimension 3 (cusp case), and Hopf bifurcation with codimension at most 2. While for system (1.4) with prey refuges, this paper showed the existence of at most three positive equilibria, three types of degenerate Bogdanov-Takens bifurcation of codimension 3 (cusp, focus and elliptic cases), and Hopf bifurcation with codimension at least 3. Moreover, we showed in Theorem 2.7 the existence of a nilpotent elliptic singularity of codimension at least 4, and system (1.4) may have a degenerate Bogdanov-Takens bifurcation of codimension at least 4 (elliptic case). Consequently, system (1.4) can have more complex dynamics, such as one or two big limit cycles enclosing one or three positive equilibria, and three kinds of homoclinic orbits (homoclinic to hyperbolic saddle, saddle-node or neutral saddle).

The prey refuge prevents prey extinction and causes the coexistence of both populations for all positive initial densities (see Lemma 2.1). The most exciting finding from our theoretical study is that refuge can induce a stable, large-amplitude limit cycle enclosing one or three positive steady states (see Fig. 3.3). This observation can potentially guide future empirical studies from the theoretical perspective. Another future effort can include Allee effect into system (1.4) [34]. Moreover, piecewise smooth systems and reaction-diffusion systems with prey refuges are useful yet challenging future directions [7,14,20,22,33].

Data availability

No data was used for the research described in the article.

Appendix A. Coefficients in the proof of Lemma 2.5

$$\phi_0 = -\frac{3}{16}(1-c^2)^4, \quad \phi_1 = \frac{3}{4}(1-c^2)^3((3c-2)(c+1)-ch(c)),$$
$$\phi_2 = -\frac{1}{4}(1-c)^2(c+1)^3(39c^3-(19h(c)+22)c^2+3(7h(c)-17)c+6(h(c)+3)),$$
$$\phi_3 = -\frac{1}{2}(1-c)(c+1)^2(2c^5+(76-7h(c))c^4+(140-51h(c))c^3-3(17h(c)+8)c^2$$
$$+3(9h(c)-26)c+6(3h(c)+2)),$$
$$\phi_4 = -\frac{1}{2}(1-c)(c+1)^2(269c^5+(472-194h(c))c^4+(412-242h(c))c^3$$
$$+(98-170h(c))c^2-3(2h(c)+35)c+36h(c)+6),$$
$$\phi_5 = -2(1-c)(c+1)^2(216c^5+(355-153h(c))c^4+(251-176h(c))c^3$$
$$+(109-105h(c))c^2-3(12h(c)+1)c+6h(c)),$$
$$\phi_6 = 2c(c+1)^2(413c^5+(467-292h(c))c^4+(52-185h(c))c^3+(21h(c)-68)c^2$$
$$+(33h(c)-81)c+39h(c)-15),$$
$$\phi_7 = 4c(c+1)^2(256c^5+(463-181h(c))c^4-3(79h(c)-99)c^3+(113-114h(c))c^2$$
$$+(23-41h(c))c-3h(c)),$$
$$\phi_8 = 4c^2(c+1)^2(99c^4+(181-70h(c))c^3-93(h(c)-1)c^2+(11-28h(c))c-h(c)).$$

Appendix B. g_1 in (4.4)

$$g_1 = [b^2(-(c^4+c^3(6z-3)+c^2(6z^2-6z+1)-3c(4z^3-6z^2+4z-1)-2(3z^2-3z+1)^2))$$
$$+2bz(c^4+c^3(5z-2)+c^2(4z-3)z+c(-6z^3+6z^2-4z+1)-2z^2(3z^2-3z+1))$$
$$+z^2(c+z)^2(-c^2-2cz+c+2z^2))]k_2^2+[2b^3(c^4+c^3(6z-3)+c^2(6z^2-6z+1)$$
$$-3c(4z^3-6z^2+4z-1)-2(3z^2-3z+1)^2)+b^2z(-6c^4+c^3(16-34z)+c^2(-42z^2$$
$$+45z-9)+3c(7z^3-2z^2+2z-1)+42z^4-51z^3+28z^2-9z+2)+bz^2(6c^4$$
$$+2c^3(16z-7)+c^2(45z^2-48z+9)+6c(z^2-6z+2)z-12z^4-6z^3+7z^2-1)$$
$$-z^3(2c^4+2c^3(5z-2)+c^2(15z^2-15z+2)+3c(2z^2-5z+1)z+2z^2(1-3z))]k_2$$
$$+b^4(-(c^4+c^3(6z-3)+c^2(6z^2-6z+1)-3c(4z^3-6z^2+4z-1)-2(3z^2-3z$$
$$+1)^2))+b^3z(4c^4+12c^3(2z-1)+c^2(34z^2-39z+9)+c(-9z^3-6z^2+2z+1)$$
$$-30z^4+39z^3-24z^2+9z-2)+b^2z^2(-6c^4+c^3(18-36z)-3c^2(21z^2-25z+6)$$
$$+c(-29z^3+86z^2-46z+7)+4z^4+33z^3-37z^2+13z-1)+bz^3(4c^4+12c^3(2z-1)$$
$$+c^2(48z^2-57z+13)+c(38z^3-85z^2+41z-6)+12z^4-46z^3+35z^2-10z+1)$$
$$-z^4(c^4+c^3(6z-3)+c^2(13z^2-15z+3)+c(12z^3-23z^2+9z-1)$$
$$+2(2z^2-5z+2)z^2).$$

Appendix C. $\bar{g}_2$ in (4.10)

$$
\begin{aligned}
\bar{g}_2 = {} & (8776581120z^{10} - 38578028544z^9 + 77610467328z^8 - 93902868480z^7 \\
& +75553310208z^6 - 42189937152z^5 + 16547268096z^4 - 4500626616z^3 + 813129552z^2 \\
& -88350696z + 4409559)b^8 + 2z(18723373056z^{10} - 72901951488z^9 + 128758628352z^8 \\
& -135093387264z^7 + 92717637120z^6 - 43202499328z^5 + 13725291952z^4 \\
& - 2904240618z^3 + 386521158z^2 - 28898361z + 942921)b^7 \\
& +z^2(68116021248z^{10} - 227134144512z^9 + 336232439808z^8 - 285490708480z^7 \\
& +149297232896z^6 - 46986569984z^5 + 7197038256z^4 + 328799476z^3 - 341448261z^2 \\
& +54194388z - 2932335)b^6 - 2z^3(34594357248z^{10} - 94284546048z^9 + 108623233024z^8 \\
& - 64649083904z^7 + 17319553280z^6 + 1670382528z^5 \\
& -2741391904z^4 + 848359354z^3 - 116772913z^2 + 5809773z + 22062)b^5 \\
& +z^4(43054006272z^{10} - 89362202624z^9 + 69225865216z^8 - 16481540096z^7 \\
& -8534749696z^6 + 6755059712z^5 - 1485851936z^4 - 63414516z^3 + 78271301z^2 \\
& -11033104z + 395721)b^4 - 2z^5(8427143168z^{10} - 11742789632z^9 \\
& +3707691008z^8 + 2479522304z^7 - 1937577472z^6 + 218092288z^5 + 171817808z^4 \\
& -58201542z^3 + 3657712z^2 + 601553z - 34695)b^3 \\
& +z^6(4063232000z^{10} - 2785869824z^9 - 1170518016z^8 + 1380023296z^7 - 51970816z^6 \\
& -219785216z^5 + 50596272z^4 + 6673164z^3 - 2542603z^2 + 84324z - 81)b^2 \\
& -2z^8(276299776z^9 + 12058624z^8 - 144109568z^7 + 12131840z^6 + 31872000z^5 \\
& -4842944z^4 - 2582432z^3 + 594230z^2 - 4053z + 27)b + (32505856z^8 + 25755648z^7 \\
& -7094272z^6 - 7556096z^5 + 1326336z^4 + 515840z^3 - 84672z^2 - 14292z + 27)z^{10}.
\end{aligned}
$$

Appendix D. w_{11}, $\chi_1(z)$, $\chi_2(z)$ in (4.15), w_{12} in (4.16)

$$
\begin{aligned}
w_{11} = {} & (234264586241861222240z^{24} - 2395476516523946803200z^{23} \\
& +11890065498919088947200z^{22} - 38111771811238222233600z^{21} \\
& +88329724024530036326400z^{20} - 156787377882564604723200z^{19} \\
& +220116914267341455360000z^{18} - 249000652196126675435520z^{17} \\
& +229337884641677153402880z^{16} - 172826777169388634112000z^{15} \\
& +106620525156128532725760z^{14} - 53652373153850861813760z^{13} \\
& +21839436238866901893120z^{12} - 7089531474935757537280z^{11} \\
& +1795554399263132917760z^{10} - 344370027730700257280z^9
\end{aligned}
$$

$$+4903156906042998784z^{8} - 5861176834750798 08z^{7} + 99427743424933200z^{6}$$
$$-24497616500969796z^{5} + 4849014898953117z^{4} - 625197123602478z^{3}$$
$$+49348725668613z^{2} - 2182224291840z + 42855402240)b^{2}$$
$$-2z(8991542209161461760z^{24} - 84008933588132167680z^{23}$$
$$+384151528666331873280z^{22} - 1148583564616862269440z^{21}$$
$$+2515455946729570959360z^{20} - 4258182605223934033920z^{19}$$
$$+5714457248139111825408z^{18} - 6140121884871974977536z^{17}$$
$$+5283044042445605044224z^{16} - 3606116644004164534272z^{15}$$
$$+1904378379124856586240z^{14} - 728690302594086862848z^{13}$$
$$+158038909134040793088z^{12} + 19504195764358651904z^{11}$$
$$-35653252213322285056z^{10} + 18077883567884896768z^{9}$$
$$-5927783457311641472z^{8} + 1401459071620339296z^{7} - 244886253416466768z^{6}$$
$$+31620699546846768z^{5} - 2999504827526463z^{4} + 209762329050702z^{3}$$
$$-10941159880143z^{2} + 399416883840z - 7142567040)b$$
$$-(2450943359708037120z^{23} - 17751527269513297920z^{22} + 61857226754956984320z^{21}$$
$$-145477949587917373440z^{20} + 274314732965084528640z^{19}$$
$$-445729837367458529280z^{18} + 616235008162403450880z^{17}$$
$$-695786945904774217728z^{16} + 622243193077547139072z^{15}$$
$$-432528435287433412608z^{14} + 229303458476788285440z^{13}$$
$$-89461884839063453696z^{12} + 23375600808009531392z^{11} - 2640905404308062208z^{10}$$
$$-763397271338147840z^{9} + 458414038903626752z^{8} - 110986676022091008z^{7} +$$
$$13895303028156288z^{6} - 370610960769504z^{5} - 158598403944732z^{4}$$
$$+26304652234053z^{3} - 2114325096246z^{2} + 122698133613z - 4761711360)z^{3},$$
$$w_{12} = 234264586241861222 40z^{24} - 239547651652394680320z^{23}$$
$$+1189006549891908894720z^{22} - 3811177181123822223360z^{21}$$
$$+8832972402453003632640z^{20} - 15678737788256460472320z^{19}$$
$$+22011691426734145536000z^{18} - 24900065219612667543552z^{17}$$
$$+22933788464167715340288z^{16}$$
$$-17282677716938863411200z^{15} + 10662052515612853272576z^{14}$$
$$-5365237315385086181376z^{13} + 2183943623886690189312z^{12}$$
$$-708953147493575753728z^{11} + 179555439926313291776z^{10}$$

$$
\begin{aligned}
&-3443700277307002572 8z^9+4903156906042998784z^8\\
&-5861176834750798 08z^7+9942774342493320 0z^6-2449761650096979 6z^5\\
&+4849014898953117z^4-625197123602478z^3+49348725668613z^2-2182224291840z\\
&+42855402240.
\end{aligned}
$$

$$
\begin{aligned}
\chi_1(z)=(&-474989023199232000z^{21}+4064718566027427840z^{20}\\
&-15488353008038707200z^{19}+34741179567518515200z^{18}\\
&-50705115335035453440z^{17}+49583767062734438400z^{16}\\
&-31132257206340157440z^{15}+9342382202903592960z^{14}\\
&+3249939501895647232z^{13}-5575105479811530752z^{12}+3378053074588270592z^{11}\\
&-1211848655616606208z^{10}+236485401248530432z^9+4916450328772608z^8\\
&-18854957774372864z^7+5860068128206848z^6-807449380339712z^5\\
&+7931592235968z^4+13085757187920z^3-1530580384584z^2+43445578770z\\
&+55801305)z,
\end{aligned}
$$

$$
\begin{aligned}
\chi_2(z)=\;&579486608303063040z^{21}-4967197710105968640z^{20}+18120534366911201280z^{19}\\
&-35204201093844172800z^{18}+32060084544098795520z^{17}\\
&+15024127774178672640z^{16}-93383699644463185920z^{15}\\
&+154828857055956172800z^{14}-161466376117781790720z^{13}\\
&+119470802979377905664z^{12}-64004616456578793472z^{11}\\
&+23580295564364873728z^{10}-4476147910404472832z^9\\
&-888228346786250752z^8+1086259263135006720z^7-465478782183497728z^6\\
&+126043498480507392z^5-23170887880897408z^4+2842342069239312z^3\\
&-215925026966064z^2+8708026419810z-140293283445.
\end{aligned}
$$

References

[1] A. Arsie, C. Kottegoda, C. Shan, A predator-prey system with generalized Holling type IV functional response and Allee effects in prey, J. Differ. Equ. 309 (2022) 704–740.

[2] A. Arsie, C. Kottegoda, C. Shan, High codimension bifurcations of a predator–prey system with generalized Holling type III functional response and Allee effects, J. Dyn. Differ. Equ. (2022), https://doi.org/10.1007/s10884-022-10214-6.

[3] M.A. Aziz-Alaoui, M.D. Okiye, Boundedness and global stability for a predator-prey model with modeled Leslie-Gower and Holling-type II schemes, Appl. Math. Lett. 16 (7) (2003) 1069–1075.

[4] J.H. Connell, Community interactions on marine rocky intertidal shores, Annu. Rro. Ecol. Syst. 3 (1972) 169–192.

[5] F. Chen, L. Chen, X. Xie, On a Leslie-Gower predator-prey model incorporating a prey refuge, Nonlinear Anal-Real. 10 (5) (2009) 2905–2908.

[6] S.N. Chow, J.K. Hale, Methods of Bifurcation Theory, Springer-Verlag, New York, 1982.

[7] X. Chen, L. Huang, A Filippov system describing the effect of prey refuge use on a ratio-dependent predator-prey model, J. Math. Anal. Appl. 428 (2) (2015) 817–837.

[8] X. Chen, W. Zhang, Decomposition of algebraic sets and applications to weak centers of cubic systems, J. Comput. Appl. Math. 23 (2009) 565–581.
[9] F. Dumortier, R. Roussarie, J. Sotomayor, Generic 3-parameter families of vector fields on the plane, unfolding a singularity with nilpotent linear part. The cusp case of codimension 3, Ergod. Theory Dyn. Syst. 7 (1987) 375–413.
[10] F. Dumortier, R. Roussarie, J. Sotomayor, K. Zoladek, Bifurcation of Planar Vector Fields, Nilpotent Singularities and Abelian Integrals, Lecture Notes in Mathematics, vol. 1480, Springer-Verlag, Berlin, 1991.
[11] H.I. Freedman, R.M. Mathsen, Persistence in predator-prey systems with ratio-dependent predator influence, Bull. Math. Biol. 55 (1993) 817–827.
[12] A. Gasull, R.E. Kooij, J. Torregrosa, Limit cycles in the Holling-Tanner model, Publ. Mat. 41 (1997) 149–167.
[13] G. Gause, N. Smaragdova, A. Witt, Further studies of interaction between predators and prey, J. Anim. Ecol. 5 (1) (1936) 1–18.
[14] R. Han, L.N. Guin, B. Dai, Consequences of refuge and diffusion in a spatiotemporal predator-prey model, Nonlinear Anal-Real. 60 (2021) 103311.
[15] J. Huang, Y. Gong, S. Ruan, Bifurcation analysis in a predator-prey model with constants-yield predator harvesting, Discrete Contin. Dyn. Syst., Ser. B 18 (2013) 2101–2121.
[16] J. Huang, S. Ruan, J. Song, Bifurcations in a predator-prey system of Leslie type with generalized Holling type III functional response, J. Differ. Equ. 257 (6) (2014) 1721–1752.
[17] S.B. Hsu, T.W. Huang, Global stability for a class of predator-prey system, SIAM J. Appl. Math. 55 (1995) 763–783.
[18] T.K. Kar, Stability analysis of a prey predator model incorporating a prey refuge, Commun. Nonlinear Sci. Numer. Simul. 10 (2005) 681–691.
[19] D.E. Knuth, The Art of Computer Programming, Seminumerical Algorithms, vol. 2, Addison-Wesley, London, 1969.
[20] W. Ko, K. Ryu, Qualitative analysis of a predator–prey model with Holling type II functional response incorporating a prey refuge, J. Differ. Equ. 231 (2) (2006) 534–550.
[21] C. Li, J. Li, Z. Ma, Codimension 3 B-T bifurcations in an epidemic model with a nonlinear incidence, Discrete Contin. Dyn. Syst., Ser. B 20 (2015) 1107–1116.
[22] W. Li, L. Huang, J. Wang, Global asymptotical stability and sliding bifurcation analysis of a general Filippove-type predator-prey model with a refuge, Appl. Math. Comput. 405 (2021) 126263.
[23] X. Li, J. Song, Global stability of a predator-prey model with modified Leslie-Gower and Holling-type schemes, Preprint.
[24] M. Lu, J. Huang, H. Wang, An organizing center of codimension four in a predator-prey model with generalist predator: from tristability and quadristability to transients in a nonlinear environmental change, SIAM J. Appl. Dyn. Syst. (2022), in press.
[25] W.W. Murdoch, A. Oaten, Predation and population stability, Adv. Ecol. Res. 9 (1975) 1–31.
[26] Z. Ma, W. Li, Y. Zhao, W. Wang, H. Zhang, Z. Li, Effects of prey refuges on a predator-prey model with a class of functional response: the role of refuges, Math. Biosci. 218 (2009) 672–683.
[27] J.N. McNair, The effects of refuges on predator-prey dynamics: a reconsideration, Theor. Popul. Biol. 29 (1986) 38–63.
[28] J.N. McNair, Stability effects of prey refuges with entry-exit dynamics, J. Theor. Biol. 125 (1987) 449–464.
[29] E. González-Olivares, R.R. Jiliberto, Dynamic consequences of prey refuges in a simple model system: more prey, fewer predators and enhanced stability, Ecol. Model. 166 (2003) 135–146.
[30] E. Sáez, E. González-Olivares, Dynamics of a predator-prey model, SIAM J. Appl. Math. 59 (1999) 1867–1878.
[31] A. Singh, H. Wang, W. Morrison, H. Weiss, Modeling fish biomass structure at near pristine coral reefs and degradation by fishing, J. Biol. Syst. 20 (2012) 21–36.
[32] S. Slimani, P.R.D. Fitte, I. Boussaada, Dynamics of a prey-predator system with modified Leslie-Gower and Holling type II schemes incorporating a prey refuge, Discrete Contin. Dyn. Syst., Ser. B 24 (9) (2019) 5003–5039.
[33] S. Tang, J. Liang, Global qualitative analysis of a non-smooth Gause predator-prey model with a refuge, Nonlinear Anal. 76 (2013) 165–180.
[34] M. Verma, A.K. Misra, Modeling the effect of prey refuge on a ratio-dependent predator-prey system with the Allee effect, Bull. Math. Biol. 80 (2018) 626–656.
[35] H. Wang, S. Thanarajah, P. Gaudreau, Refuge-mediated predator-prey dynamics and biomass pyramids, Math. Biosci. 298 (2018) 29–45.
[36] H. Wang, W. Morrison, A. Singh, H. Weiss, Modeling inverted biomass pyramids and refuges in ecosystems, Ecol. Model. 220 (2009) 1376–1382.
[37] C. Xiang, J. Huang, S. Ruan, D. Xiao, Bifurcation analysis in a host-generalist parasitoid model with Holling II functional response, J. Differ. Equ. 268 (8) (2019) 4618–4662.

[38] C. Xiang, J. Huang, H. Wang, Linking bifurcation analysis of Holling-Tanner model with generalist predator to a changing environment, Stud. Appl. Math. 149 (2022) 124–163.
[39] L. Yang, Recent advances on determining the number of real roots of parametric polynomials, J. Symb. Comput. 28 (1999) 225–242.
[40] Z. Zhang, T. Ding, W. Huang, Z. Dong, Qualitative Theory of Differential Equations, Transl. Math. Monogr., vol. 101, Amer. Math. Soc., Providence, RI, 1992.